Fundamentals of RF Cavities

Suba De Silva, S. A. Bogacz, G. A. Krafft,
and R. Gamage
Old Dominion University / Jefferson Lab
Colorado State University

Lecture 10

Outline

- RF Cavities
  - Cavity Basics
  - RF Properties
  - TM Type Cavities
- Types of Cavities
  - Accelerating Cavities
  - Low β cavities
  - Deflecting/Crabbing Cavities
- Limitations in SRF Cavities
- Losses in RF Cavities

Suggested Literature

- H. Padamsee, J. Knobloch, T. Hays “ RF Superconductivity for Accelerators”, John Wiley & Sons, Inc; ISBN 0-471-15432-6
- Proceedings of the Workshops on RF Superconductivity 1981–2015 – (ww.jacow.org)
- CERN Accelerator School – 1955 – 2016 (https://cds.cern.ch/collection/CERN%20Yellow%20Reports?ln=en)

RF Cavities

RF cavities made of different materials, in different shapes and sizes


CESR 500 MHz Cavity (Cornell)


LEP 350 MHz 4-cell Nb on Cu


1500 MHz 5-cell

1300 MHz 9-cell

Quarter Wave Cavity

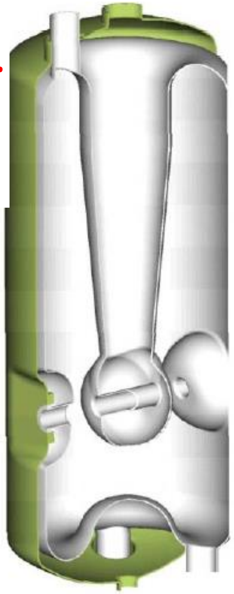

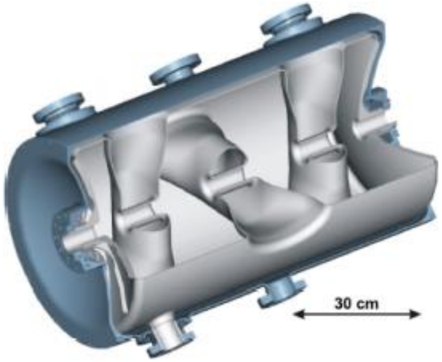

Triple Spoke Cavity

Half Wave Cavity

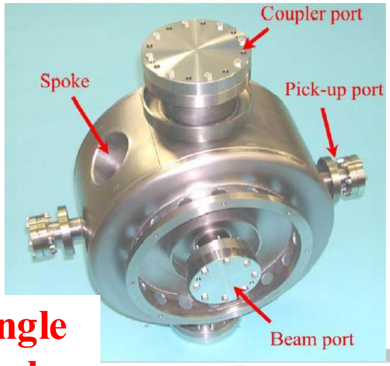

Single Spoke Cavity

RF Cavities

- Space enclosed by conducting walls that can sustain an infinite number of resonant electromagnetic modes

- Shape is selected so that a particular mode can efficiently transfer its energy to a charged particle

- An isolated mode can be modeled by an LRC circuit

- Lorentz force $\vec{F} = q(\vec{E} + \vec{v} \times \vec{B})$

- An accelerating cavity needs to provide an electric field (E) longitudinal with the velocity of the particle
- Magnetic fields (H) provide deflection but no acceleration

RF Resonator

- Simplest form of RF resonator → LC circuit

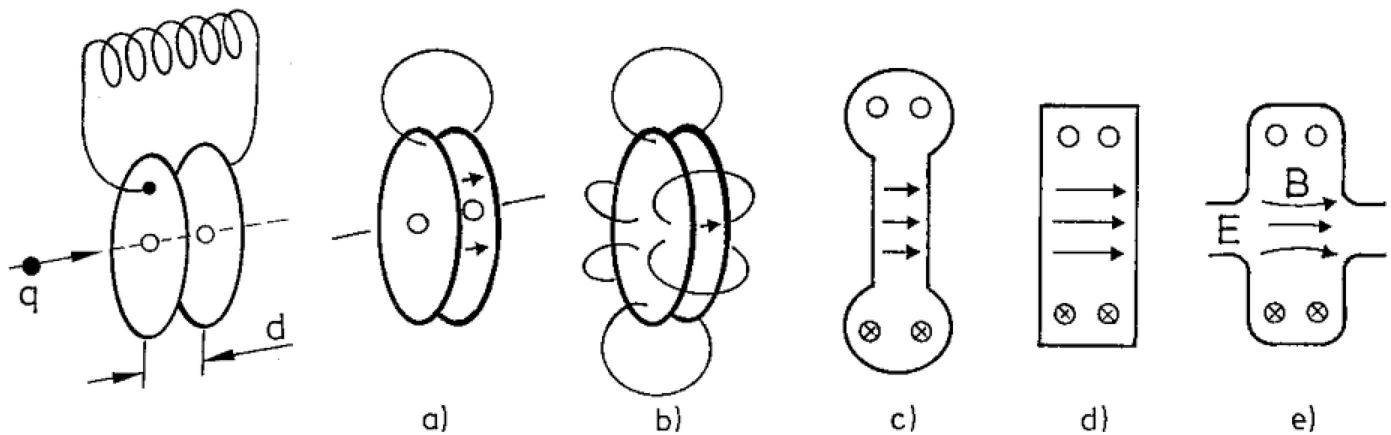

- LC circuit → Pill box cavity
  - Electric field is concentrated near axis
  - Magnetic field is concentrated at outer cylindrical wall

Cavity Basics

- Fields in an rf cavity are solution to the wave equation

$$\left(\nabla^2 - \frac{1}{c}\frac{\partial^2}{\partial t}\right)\begin{Bmatrix}\mathbf{E}\\ \mathbf{H}\end{Bmatrix} = 0$$

- Subjected to boundary conditions:
  – No tangential electric field $\hat{n}\times\mathbf{E} = 0,$
  – No normal magnetic field $\hat{n}\cdot\mathbf{H} = 0$

- Two sets of eigenmode solutions with infinite number of modes
  – TM modes → Modes with longitudinal electric fields and no transverse magnetic fields
  – TE modes → Modes with longitudinal magnetic fields and no transverse electric fields

TM and TE Modes in a Pill Box Cavity

TM Modes:
$$\begin{cases} E_z = E_0 \cos\left(\frac{p\pi z}{L}\right) J_m\left(\frac{x_{mn} r}{R}\right)\cos(m\phi)\,, \\ E_r = -E_0 \frac{p\pi R}{L x_{mn}} \sin\left(\frac{p\pi z}{L}\right) J'_m\left(\frac{x_{mn} r}{R}\right)\cos(m\phi)\,, \\ E_\phi = E_0 \frac{m p \pi R^2}{r L x_{mn}^2} \sin\left(\frac{p\pi z}{L}\right) J_m\left(\frac{x_{mn} r}{R}\right)\sin(m\phi)\,, \\ H_z = 0\,, \\ H_r = j E_0 \frac{m\omega R^2}{c\eta r x_{mn}^2} \cos\left(\frac{p\pi z}{L}\right) J_m\left(\frac{x_{mn} r}{R}\right)\sin(m\phi)\,, \\ H_\phi = j E_0 \frac{\omega R}{c\eta x_{mn}} \cos\left(\frac{p\pi z}{L}\right) J'_m\left(\frac{x_{mn} r}{R}\right)\cos(m\phi)\,, \end{cases}$$

$$\omega_{TM_{mnp}} = c\sqrt{\left(\frac{x_{mn}c}{R}\right)^2 + \left(\frac{p\pi}{L}\right)^2}\,,$$

TE Modes:
$$\begin{cases} H_z = H_0 \sin\left(\frac{p\pi z}{L}\right) J_m\left(\frac{x'_{mn} r}{R}\right)\cos(m\phi)\,, \\ H_r = H_0 \frac{p\pi R}{L x'_{mn}} \cos\left(\frac{p\pi z}{L}\right) J'_m\left(\frac{x'_{mn} r}{R}\right)\cos(m\phi)\,, \\ H_\phi = -H_0 \frac{m p \pi R^2}{r L (x'_{mn})^2} \cos\left(\frac{p\pi z}{L}\right) J_m\left(\frac{x'_{mn} r}{R}\right)\sin(m\phi)\,, \\ E_z = 0\,, \\ E_r = j H_0 \frac{m\eta\omega R^2}{c r (x'_{mn})^2} \sin\left(\frac{p\pi z}{L}\right) J_m\left(\frac{x'_{mn} r}{R}\right)\sin(m\phi)\,, \\ E_\phi = j H_0 \frac{\eta\omega R}{c x'_{mn}} \sin\left(\frac{p\pi z}{L}\right) J'_m\left(\frac{x'_{mn} r}{R}\right)\cos(m\phi)\,, \end{cases}$$

$$\omega_{TE_{mnp}} = c\sqrt{\left(\frac{x'_{mn}c}{R}\right)^2 + \left(\frac{p\pi}{L}\right)^2}\,.$$

x_{mn} is the n^th^ root of J_m
x'_{mn} is the n^th^ root of J'_m

Modes in Pill Box Cavity

- TM_{010}
  - Electric field is purely longitudinal
  - Electric and magnetic fields have no angular dependence
  - Frequency depends only on radius, independent on length
- TM_{0np}
  - Monopole modes that can couple to the beam and exchange energy
- TM_{1np}
  - Dipole modes that can deflect the beam
- TE modes
  - No longitudinal *E* field
  - Cannot couple to the beam
  - TE-type modes can deflect the beam

Pill Box Cavity

- Needs longitudinal electric field for acceleration
- Operated in the TM_{010} mode
- Hollow right cylindrical enclosure

TM_{010} mode

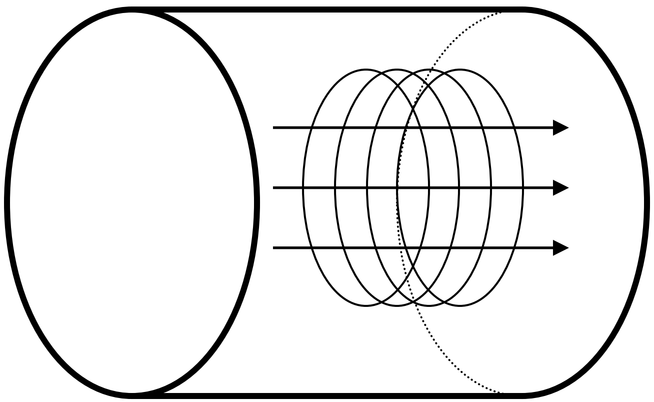

$$\frac{\partial^2 E_z}{\partial^2 r} + \frac{1}{r}\frac{\partial E_z}{\partial r} = \frac{1}{c^2}\frac{\partial^2 E_z}{\partial^2 t} \qquad \omega_0 = \frac{2.405c}{R}$$

$$E_z(r,z,t) = E_0 J_0\left(2.405\frac{r}{R}\right)e^{-i\omega_0 t}$$

$$H_\varphi(r,z,t) = -i\frac{E_0}{\mu_0 c}J_1\left(2.405\frac{r}{R}\right)e^{-i\omega_0 t}$$

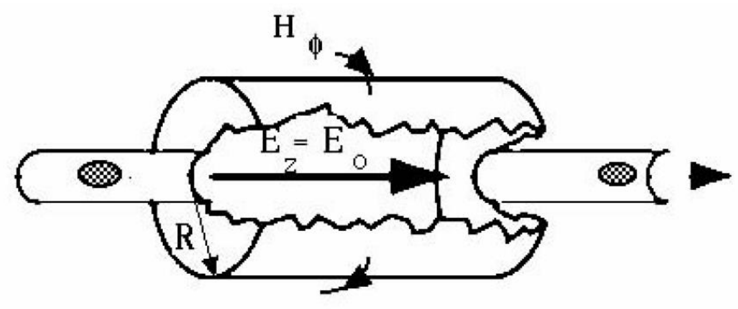

TM_{010} Mode in a Pill Box Cavity

$$E_r = E_\varphi = 0 \qquad E_z = E_0 J_0\left(x_{01}\frac{r}{R}\right)$$

$$H_r = H_z = 0 \qquad H_\varphi = -i\omega\varepsilon E_0 \frac{R}{x_{01}} J_1\left(x_{01}\frac{r}{R}\right)$$

$$\omega = x_{01}\frac{c}{R} \qquad x_{01} = 2.405$$

$$R = \frac{x_{01}}{2\pi}\lambda = 0.383\lambda$$

TM_{010} mode

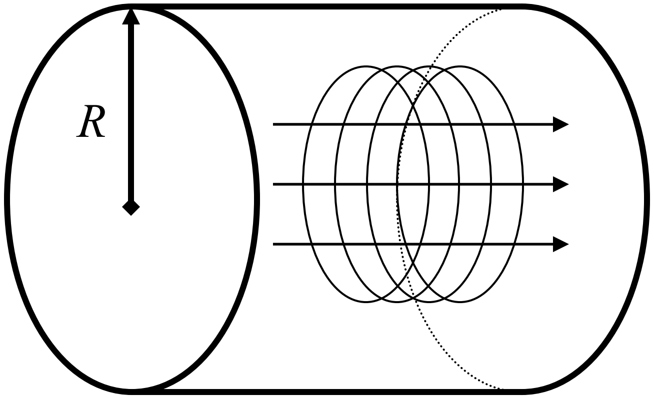

- Frequency scales inversely with cavity radius

TM$_{010}$ Field Profile

Electric Field

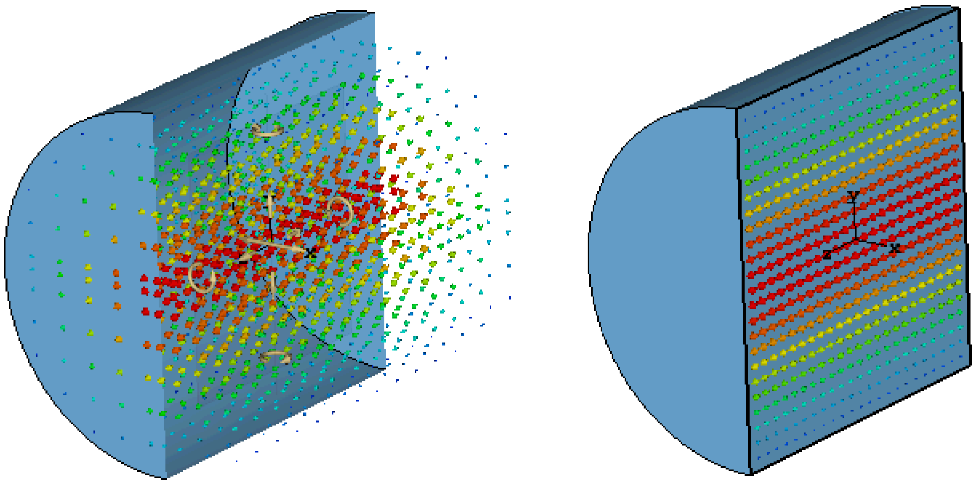

Surface Electric Field

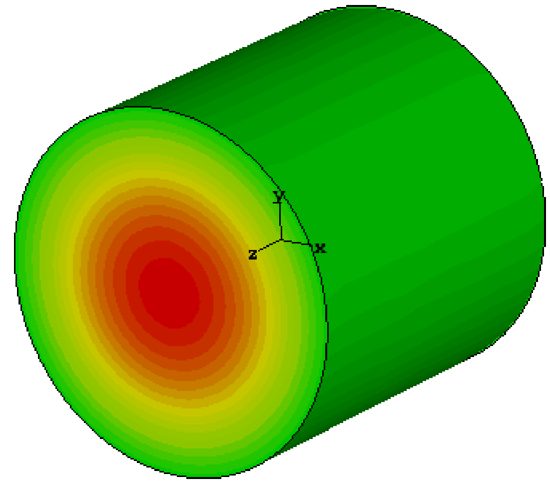

Magnetic Field

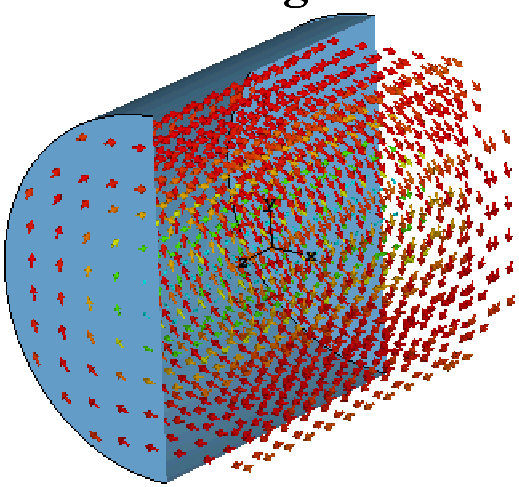

- Peak surface electric field at end plates
- Peak surface magnetic field at outer cylindrical surface

Surface Magnetic Field

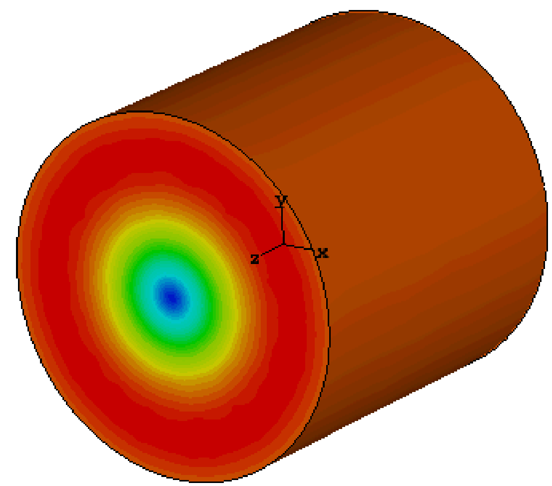

Cavity RF Properties

Accelerating Voltage

- For efficient acceleration, choose a cavity geometry and a mode where:
  - Electric field is along the particle trajectory
  - Magnetic field is zero along the particle trajectory
  - Velocity of the electromagnetic field is matched to particle velocity

- Accelerating voltage for charged particles

$$V_c = \left| \int_{-\infty}^{\infty} E_z(\rho = 0, z) e^{i\omega_0 z/\beta c} dz \right|$$

Accelerating Voltage (V_c)

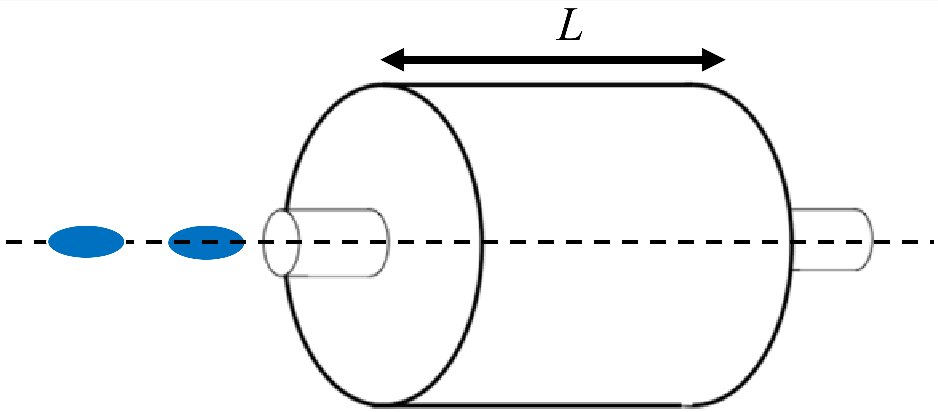

$$L = \frac{\beta\lambda}{2}$$

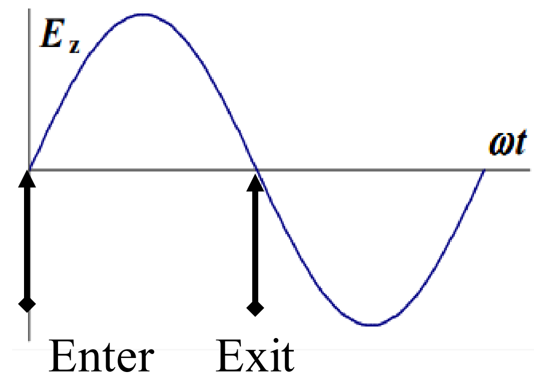

- Accelerating voltage for charged particles

$$V_c = \left| \int_{-\infty}^{\infty} E_z(\rho = 0, z) e^{i\omega_0 z/\beta c} dz \right|$$

- For the pill box cavity

$$V_c = E_0 \left| \int_0^d e^{i\omega_0 z/\beta c} dz \right| = E_0 d \frac{\sin\left(\frac{\omega_0 d}{2\beta c}\right)}{\frac{\omega_0 d}{2\beta c}} = E_0 d \cdot T$$

T is the transit time factor

Accelerating Gradient (E_{acc})

- Accelerating field (gradient): Voltage gained by a particle divided by a reference length

$$E_{acc} = \frac{V_{acc}}{L}$$

- For velocity of light particles: $L = \frac{N\lambda}{2}$

  N – no. of cells

- For less-than-velocity-of-light cavities ($\beta < 1$), there is no universally adopted definition of the reference length
- However multi-cell elliptical cavities with $\beta < 1$

  Length per cell $L = \frac{\beta\lambda}{2}$

Stored Energy (U)

- Energy density in electromagnetic field:

$$u = \frac{1}{2}\left(\varepsilon_0 \mathbf{E}^2 + \mu_0 \mathbf{H}^2\right)$$

- Because of the sinusoidal time dependence and the 90º phase shift, the energy oscillates back and forth between the electric and magnetic field

- Total energy content in the cavity:

$$U = \frac{\varepsilon_0}{2}\int_V dV\,|\mathbf{E}|^2 = \frac{\mu_0}{2}\int_V dV\,|\mathbf{H}|^2$$

Power Dissipation (P_{diss})

- Surface current results in power dissipation proportional to the surface resistance (R_s)

- Power dissipation per unit area

$$\frac{dP}{da} = \frac{\mu_0 \omega \delta}{4} \left| \mathbf{H}_{\parallel} \right|^2 = \frac{R_s}{2} \left| \mathbf{H}_{\parallel} \right|^2$$

- Total power dissipation in the cavity walls

$$P = \frac{R_s}{2} \int_A da \left| \mathbf{H}_{\parallel} \right|^2$$

Power Dissipation (P_{diss})

$$\frac{P}{L} \propto \frac{1}{\frac{R}{Q} Q R_S} \frac{E^2 R_S}{\omega}$$

- For normal conductors → $R_S \propto \omega^{1/2}$
  - per unit length $\frac{P}{L} \propto \omega^{-\frac{1}{2}}$
  - per unit area $\frac{P}{A} \propto \omega^{\frac{1}{2}}$

- For superconductors → $R_S \propto \omega^2$
  - per unit length $\frac{P}{L} \propto \omega$
  - per unit area $\frac{P}{A} \propto \omega^2$

Quality Factor (Q_0)

- Measures cavity performance as to how lossy cavity material is for given stored energy

$$Q_0 \equiv \frac{\text{Energy stored in cavity}}{\text{Energy dissipated in cavity walls per radian}} = \frac{\omega_0 U}{P_{diss}}$$

$$= \omega_0 \tau_0 = \frac{\omega_0}{\Delta\omega_0}$$

$$Q_0 = \frac{\omega\mu_0}{R_s} \frac{\int_V dV \, |\mathbf{H}|^2}{\int_A da \, |\mathbf{H}_{||}|^2}$$

- For normal conducting cavities ~ 10^4
- For superconducting cavities ~ 10^{10}

Geometrical Factor (G)

- Geometrical factor [Ω]
  - Product of the qualify factor (Q_0) and the surface resistance (R_s)
  - Independent of size and material
  - Depends only on shape of cavity and electromagnetic mode
  - For superconducting elliptical cavities $QR_s \sim 275\Omega$

$$G = QR_s = \omega\mu_0 \frac{\int_V dV\, |\mathbf{H}|^2}{\int_A da |\mathbf{H}_{||}|^2} = 2\pi\sqrt{\frac{\mu_0}{\varepsilon_0}}\frac{1}{\lambda}\frac{\int_V dV\, |\mathbf{H}|^2}{\int_A da |\mathbf{H}_{||}|^2} = \frac{2\pi\eta}{\lambda}\frac{\int_V dV\, |\mathbf{H}|^2}{\int_A da |\mathbf{H}_{||}|^2}$$

$\eta \approx 377\Omega$ Impedance of vacuum

Shunt Impedance (R_{sh}) and R/Q

- Shunt impedance (R_{sh}) [Ω] $$R_{sh} \equiv \frac{V_c^2}{P_{diss}}$$

- Maximize shunt impedance to get maximum acceleration

- Note: Sometimes the shunt impedance is defined as or quoted as impedance per unit length (Ω/m) $$\frac{V_c^2}{2P_{diss}}$$

- R/Q [Ω]: Measures of how much of acceleration for a given power dissipation

$$\frac{R}{Q} = \frac{V^2}{P}\frac{P}{\omega U} = \frac{E^2}{U}\frac{L^2}{\omega}$$

$R_{sh}R_s$ and R/Q

- Optimization parameter:

$$R_{sh}R_s = \frac{R_{sh}}{Q} QR_s = \frac{R}{Q} G$$

- R/Q and $R_{sh}R_s$
  - Independent of size (frequency) and material
  - Depends on mode geometry
  - Proportional to no. of cells

- In practice for elliptical cavities
  - $R/Q \sim 100\ \Omega$ per cell
  - $R_{sh}R_s \sim 33{,}000\ \Omega^2$ per cell

TM_{010} Mode in a Pill Box Cavity

Energy content

$$U = \varepsilon_0 E_0^2 \frac{\pi}{2} J_1^2(x_{01}) L R^2$$

Power dissipation

$$P = E_0^2 \frac{R_s}{\eta^2} \pi J_1^2(x_{01})(R+L)R$$

$$x_{01} = 2.40483$$

$$J_1(x_{01}) = 0.51915$$

Geometrical factor

$$G = \eta \frac{x_{01}}{2} \frac{L}{(R+L)}$$

TM_{010} Mode in a Pill Box Cavity

Energy Gain

$$\Delta W = E_0 \frac{\lambda}{\pi} \sin \frac{\pi L}{\lambda}$$

Gradient

$$E_{acc} = \frac{\Delta W}{\lambda / 2} = E_0 \frac{2}{\pi} \sin \frac{\pi L}{\lambda}$$

Shunt impedance

$$R_{sh} = \frac{\eta^2}{R_s} \frac{1}{\pi^3 J_1^2(x_{01})} \frac{\lambda^2}{R(R+L)} \sin^2\left(\frac{\pi L}{\lambda}\right)$$

Accelerating Cavities

Real Cavities

- Beam tubes reduce the electric field on axis
  - Gradient decreases
  - Peak fields increase
  - *R*/*Q* decreases

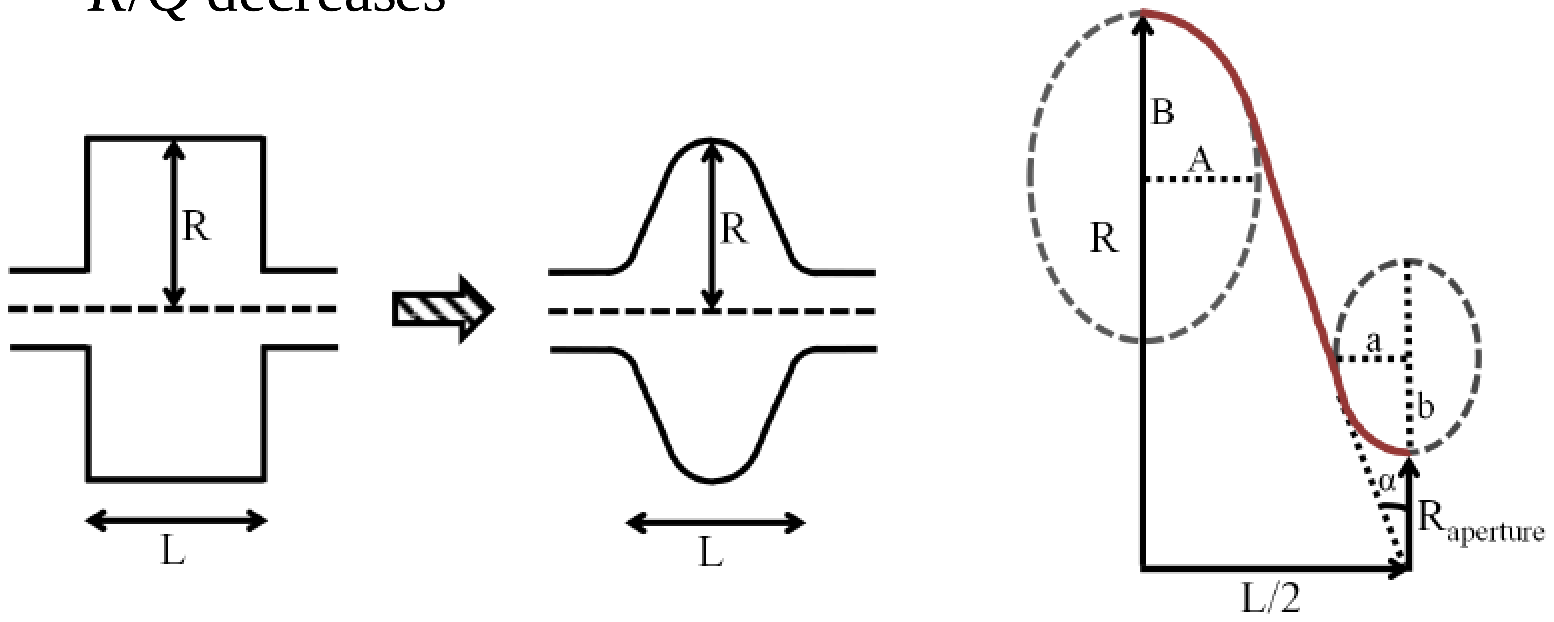

Pill Box to Elliptical Cavities

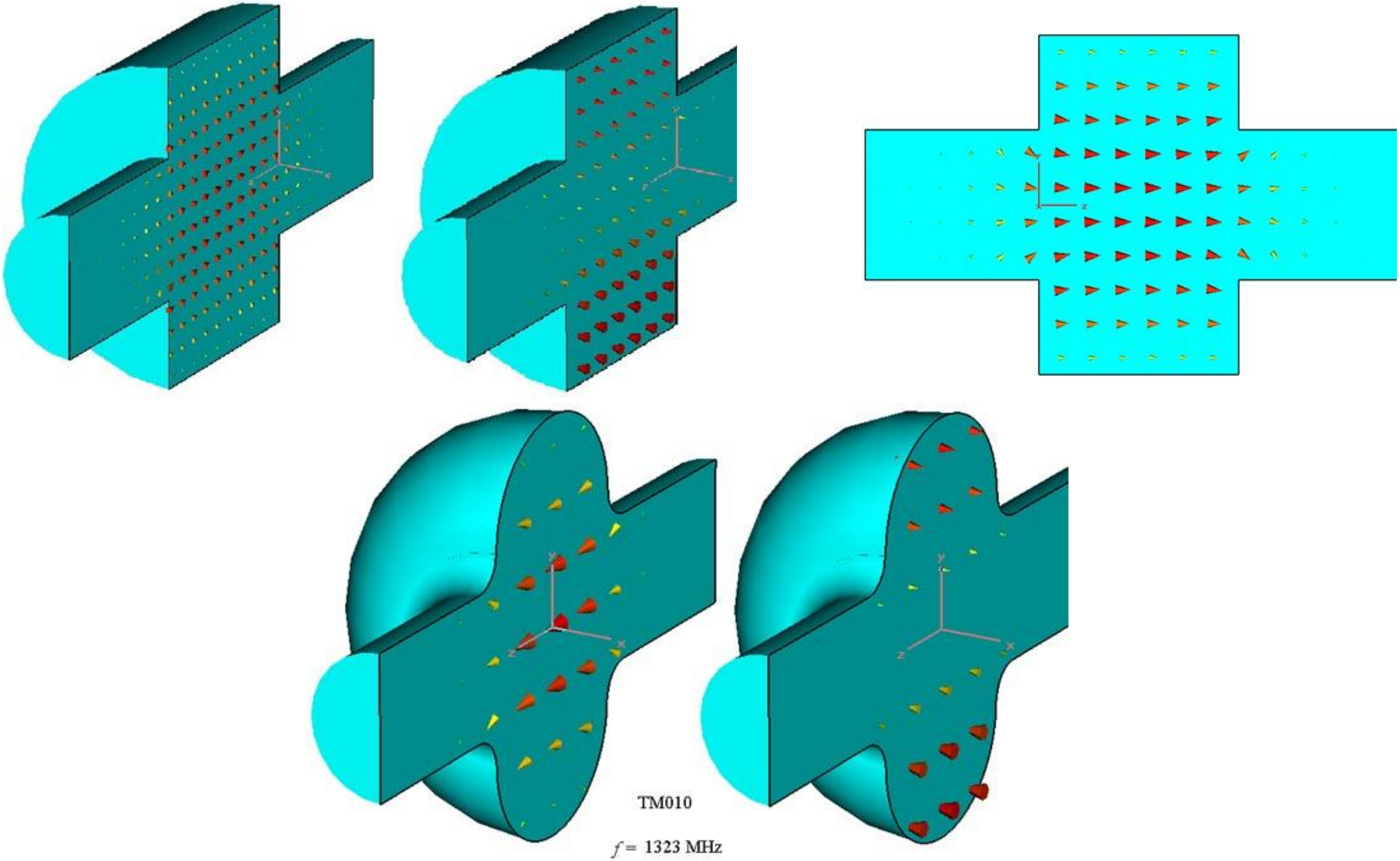

Single Cell Cavities

Electric field high at iris

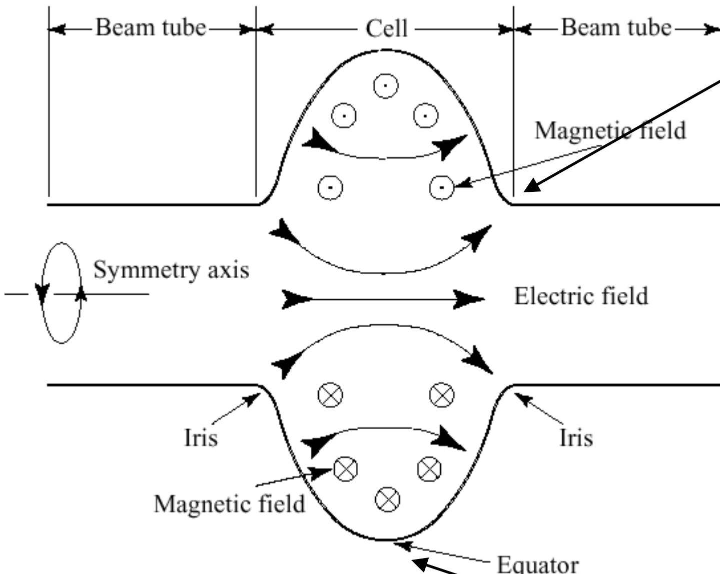

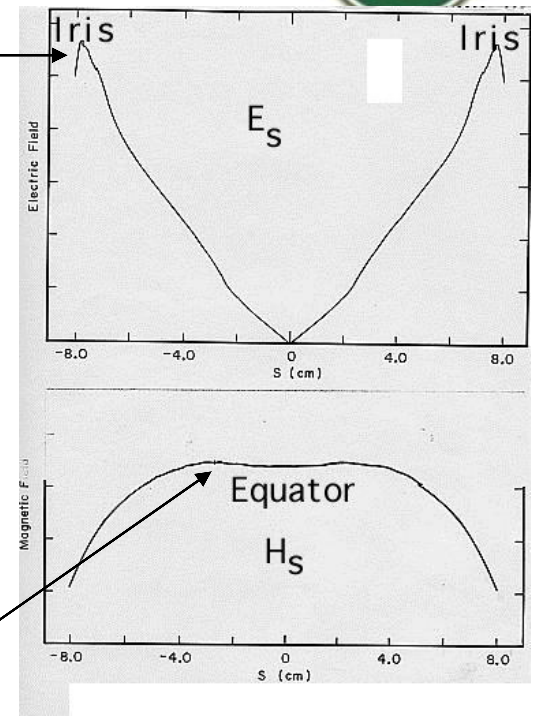

Magnetic field high at equator

- Important parameters: E_p/E_{acc} and B_p/E_{acc}
- Must minimize the ratios as smaller as possible

Single Cell Cavities

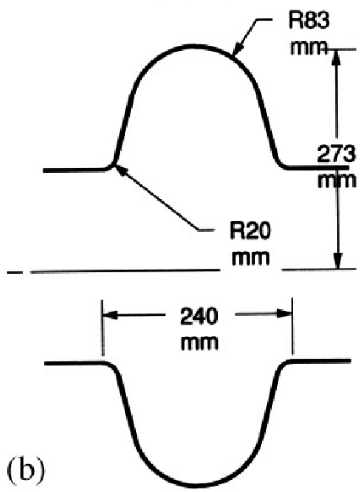

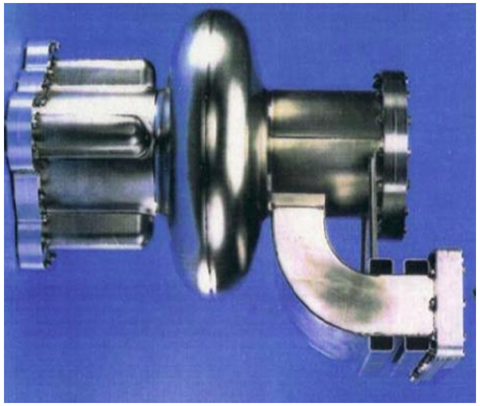

Quantity	Cornell SC 500 MHz	Pillbox
G	270 Ω	257 Ω
$R_{\rm a}/Q_0$	88 Ω/cell	196 Ω/cell
$E_{\rm pk}/E_{\rm acc}$	2.5	1.6
$H_{\rm pk}/E_{\rm acc}$	52 Oe/MV/m	30.5 Oe/(MV/m)

Cell Shape Design

- What is the purpose of the cavity?
- What EM parameters should be optimized to meet the design specs?

The "perfect" shape does not exist, it all depends on your application

- Beam aperture
- Peak surface field ratios – E_p/E_{acc}, B_p/E_{acc}
- Shunt impedance – $R_{sh}R_s$
- Higher Order Mode (HOM) extraction

Example: CEBAF Upgrade

- "High Gradient" shape: lowest E_p/E_{acc}
- "Low Loss" shape: lowest cryogenic losses $R_{sh}R_s = G(R/Q)$

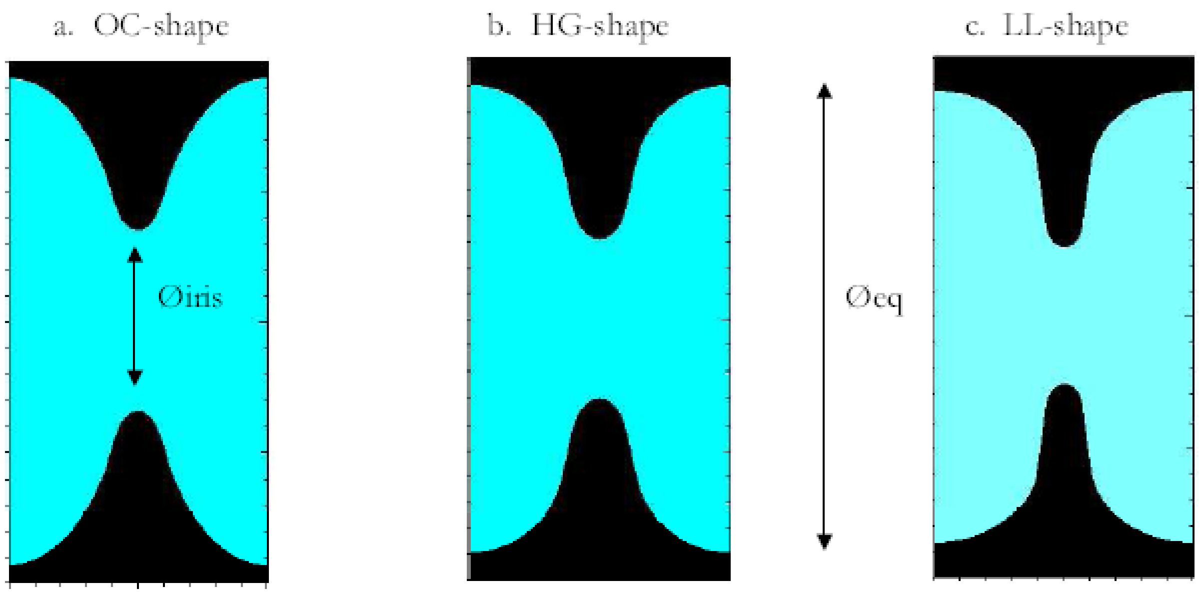

TM-Cavity Design

- The **field emission is not a hard limit** in the performance of sc cavities if the surface preparation is done in the right way

- Unlikely this, **magnetic flux on the wall** limits performance of a sc cavity (Q_0 decreases or/and quench). Hard limit ~**180 mT** for Nb

B_{peak} / E_{acc} should be low

1. Cavities may operate at higher gradients.

2. Cavities may operate at lower cryogenic load.

$$\frac{P_{diss}}{V_{acc}^2} \equiv \frac{R_s}{G \cdot (R/Q)}$$

New Shapes for ILC

f = 1300 MHz

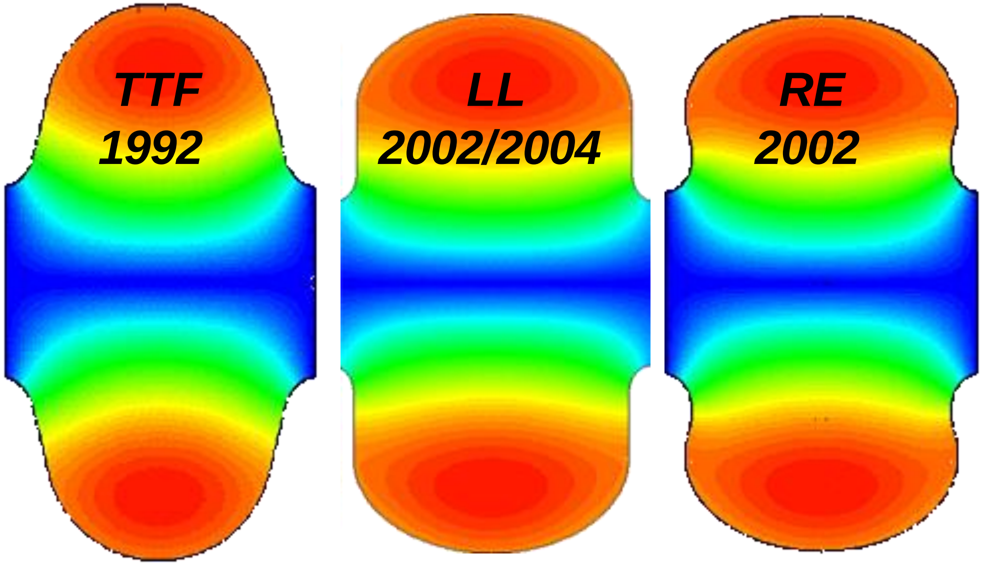

r_{iris}	[mm]	35	30	33
k_{cc}	[%]	1.9	1.52	1.8
E_{peak}/E_{acc}	-	1.98	2.36	2.21
B_{peak}/E_{acc}	[mT/(MV/m)]	4.15	3.61	3.76
R/Q	[Ω]	113.8	133.7	126.8
G	[Ω]	271	284	277
R/Q*G	[Ω*Ω]	30840	37970	35123

RF Simulation Codes for Cavity Design

The solution to 2D (or 3D) Helmholtz equation can be analytically found only for very few geometries (pillbox, spherical resonators or rectangular resonator).

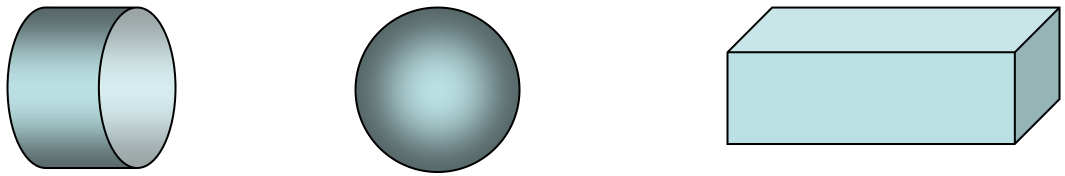

We need numerical methods:

$$(\nabla^2+\omega^2\varepsilon\mu)A=0$$

Approximating operator (Finite Difference Methods)

Approximating function (Finite Element Methods)

- 2D is fast and allows to define geometry of a cylindrical symmetric body (inner and end-cells) of the cavity.

- 3D is much more time consuming but necessary for modeling of full equipped cavity with FPC and HOM couplers and if needed to model fabrication errors. Also coupling strength for FPC and damping of HOMs can be modeled only 3D.

SUPERFISH

- Free, 2D finite-difference code to design cylindrically symmetric structures (monopole modes only)
- Use symmetry planes to reduce number of mesh points

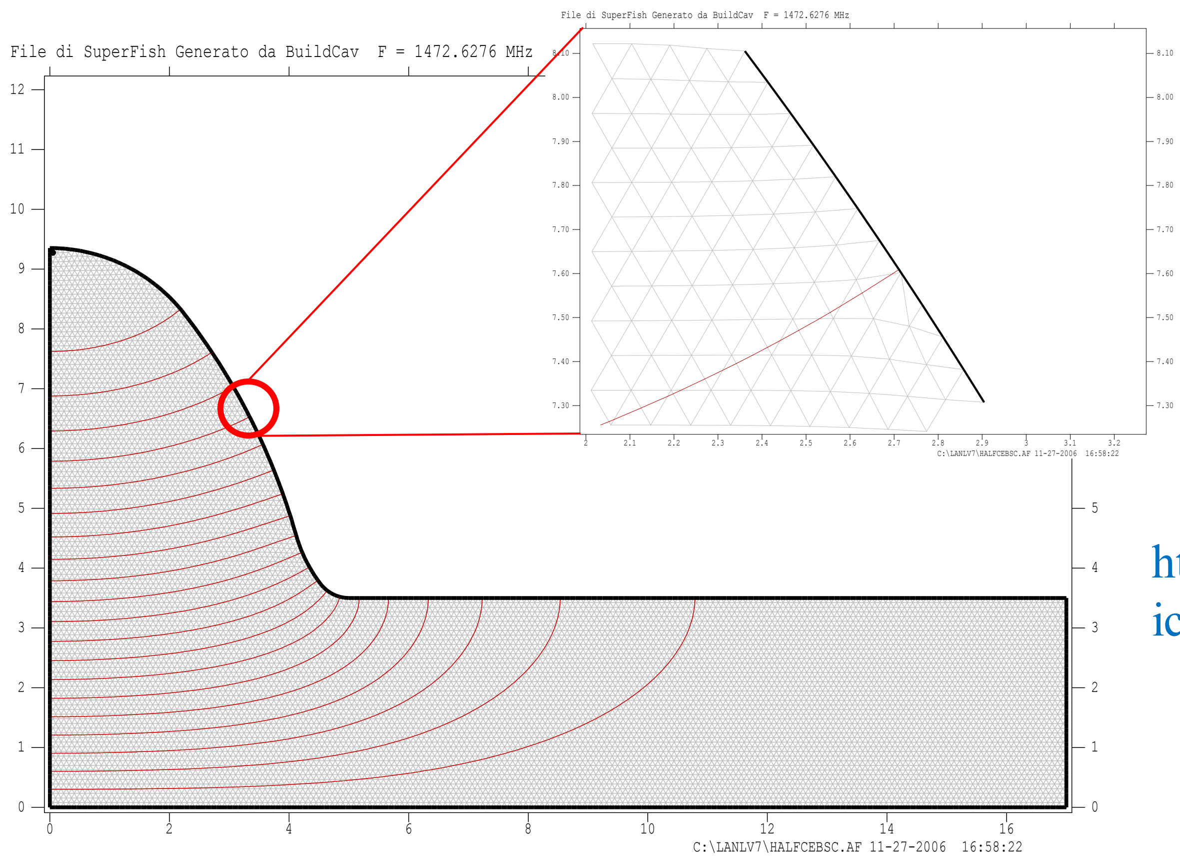

http://laacg1.lanl.gov/laacg/services/download_sf.phtml

CST Microwave Studio

- Expensive, 3D finite-element code, used to design complex RF structure
- Runs on PC
- Perfect boundary approximation

http://www.cst.com/Content/Products/MWS/Overview.aspx

Hexahedral mesh

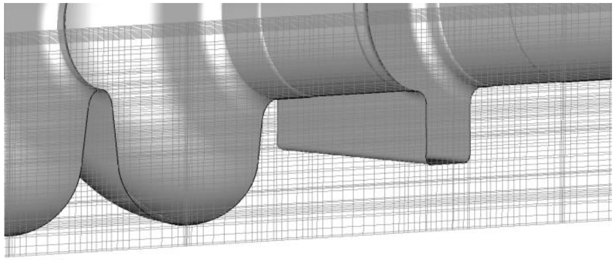

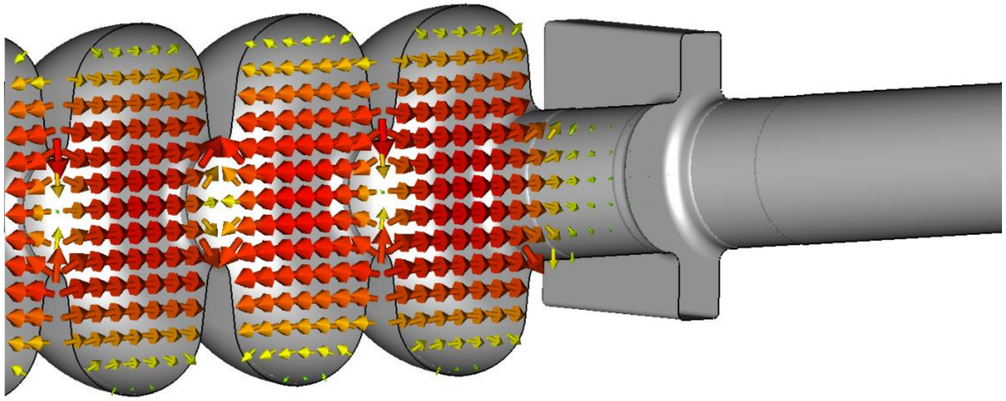

Omega3P – ACE3P (SLAC Code Suite)

- SLAC, 3D code, high-order Parallel Finite Element (PFE) method
- Runs on Linux
- Tetrahedral conformal mesh
- High order finite elements (basis order p =1 – 6)
- Separate software for user interface (Cubit), and visualization and post processing (ParaView)

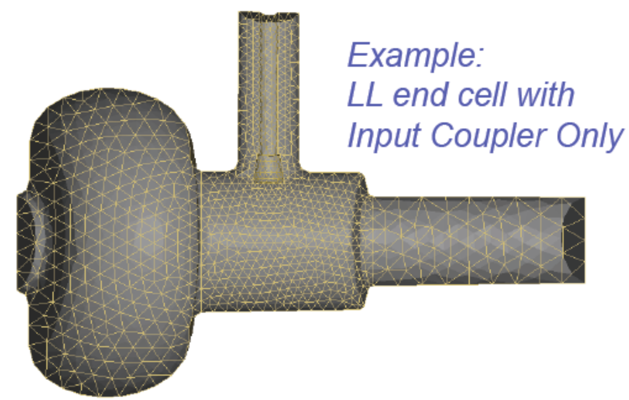

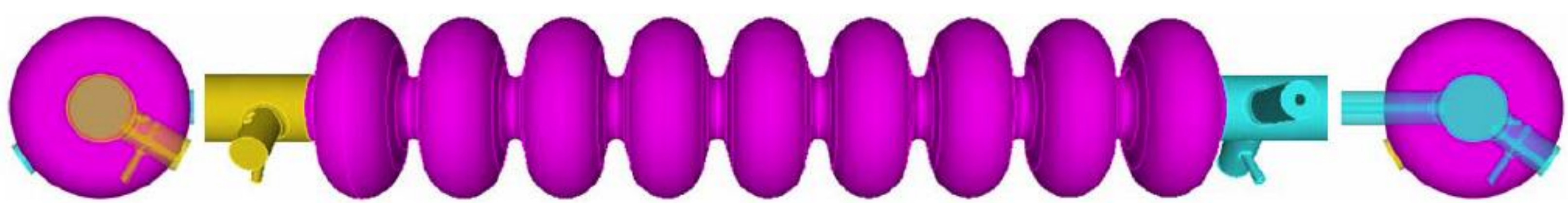

Cell Shape Parametrization

- Full parametric model of the cavity in terms of 7 meaningful geometrical parameters:
  - ✓ Ellipse ratio at the equator ($R=B/A$)
    ruled by mechanics
  - ✓ Ellipse ratio at the iris ($r=b/a$)
    E_{peak}
  - ✓ Side wall inclination (α) and position (d)
    E_{peak} vs. B_{peak} tradeoff and coupling k_{cc}
  - ✓ Cavity iris radius R_{iris}
    coupling k_{cc}
  - ✓ Half-cell Length $L/2=\lambda\beta/4$
    β
  - ✓ Cavity radius D
    used for frequency tuning
- Behavior of all EM and mechanical properties has been found as a function of the above parameters

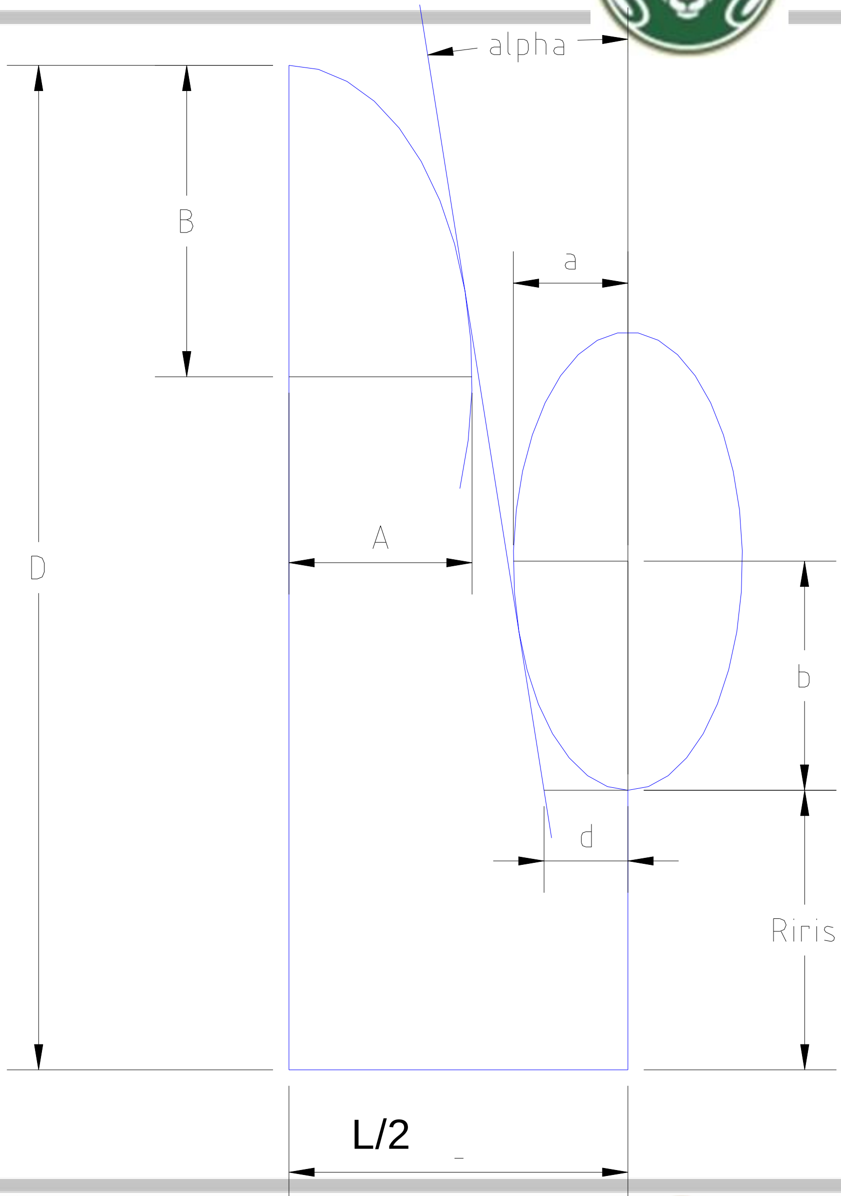

Reducing Peak Surface Fields

- "Rule of thumb" for Optimizing Peak Surface Fields

Add "*magnetic volume*" at the equator to reduce B_{peak}

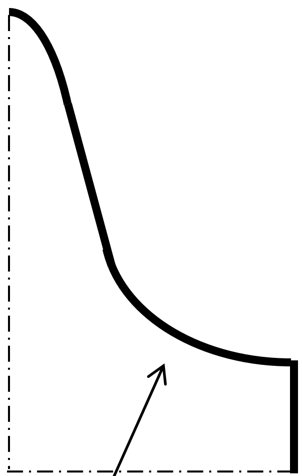

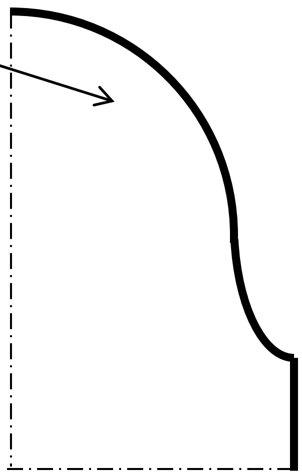

Add "*electric volume*" at the iris to reduce E_{peak}

Multi-Cell Cavities

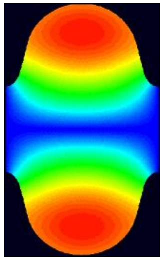

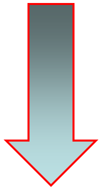

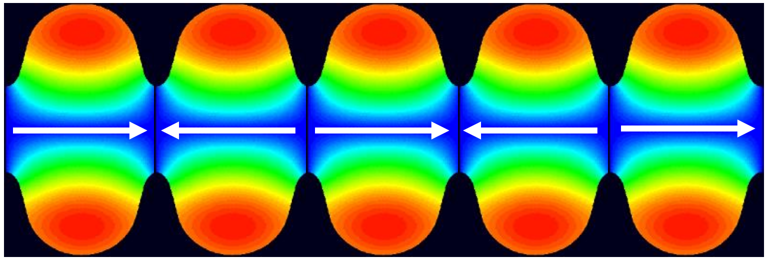

Single-cell is attractive from the RF-point of view:

- Easier to manage HOM damping
- No field flatness problem
- Input coupler transfers less power
- Easy for cleaning and preparation

- ***But it is expensive to base even a small linear accelerator on the single cell. We do it only for very high beam current machines.***

A multi-cell structure is less expensive and offers higher real-estate gradient but:

- ***Field flatness (stored energy) in cells becomes sensitive to frequency errors of individual cells***
- ***Other problems arise: HOM trapping…***

Cell to Cell Coupling

ω_o

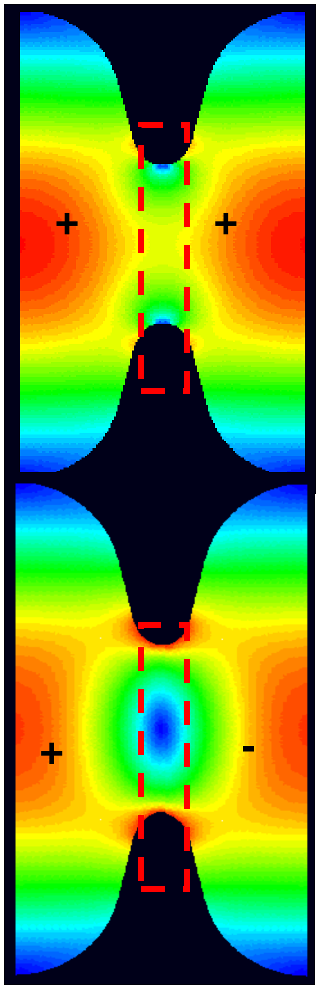

ω_π

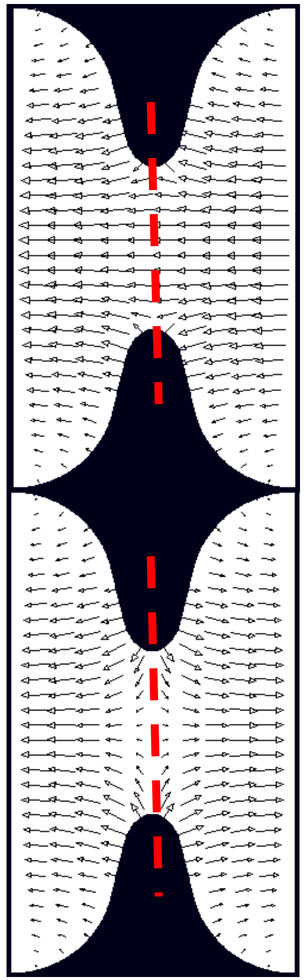

Symmetry plane for the H field

Symmetry plane for the E field which is an additional solution

The normalized difference between these frequencies is a measure of the energy flow via the coupling region

$$k_{cc} = \frac{\omega_\pi - \omega_0}{\frac{\omega_\pi + \omega_0}{2}}$$

Pros and Cons of Multi-Cell Cavities

- Cost of accelerators are lower (less auxiliaries: He vessels, tuners, fundamental power couplers, control electronics)
- Higher real-estate gradient (better fill factor)

- Field flatness vs. N (N – no. of cells)
- HOM trapping vs. N
- Power capability of fundamental power couplers vs. N
- Chemical treatment and final preparation become more complicated
- The worst performing cell limits whole multi-cell structure

Multi-Cell Cavities

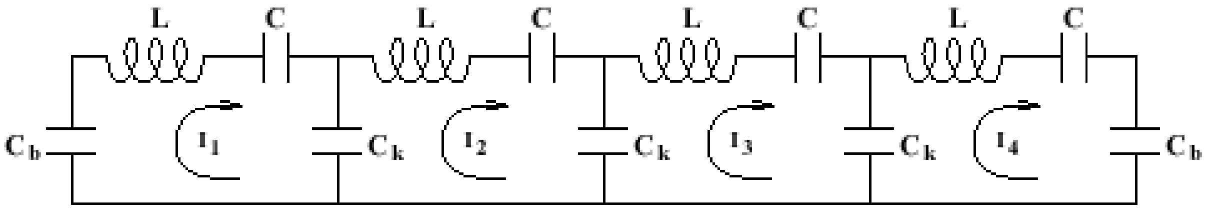

$$k = \frac{C}{C_k} \qquad C_b = C_k / 2$$

Mode frequencies:

$$\frac{\omega_m^2}{\omega_0^2} = 1 + 2k\left(1 - \cos\frac{\pi m}{n}\right)$$

$$\frac{\omega_n - \omega_{n-1}}{\omega_0} = k\left(1 - \cos\frac{\pi}{n}\right) = \frac{k}{2}\left(\frac{\pi}{n}\right)^2$$

ω_0 – accelerating mode frequency

Voltages in cells:

$$V_j^m = \sin\left(\pi m \frac{2j-1}{2n}\right)$$

Pass-Band Modes Frequencies

Coupling of TM_{010} modes of the individual cells via the iris (primarily electric field) causes them to split into a passband of closely spaced modes equal in number to the number of cells

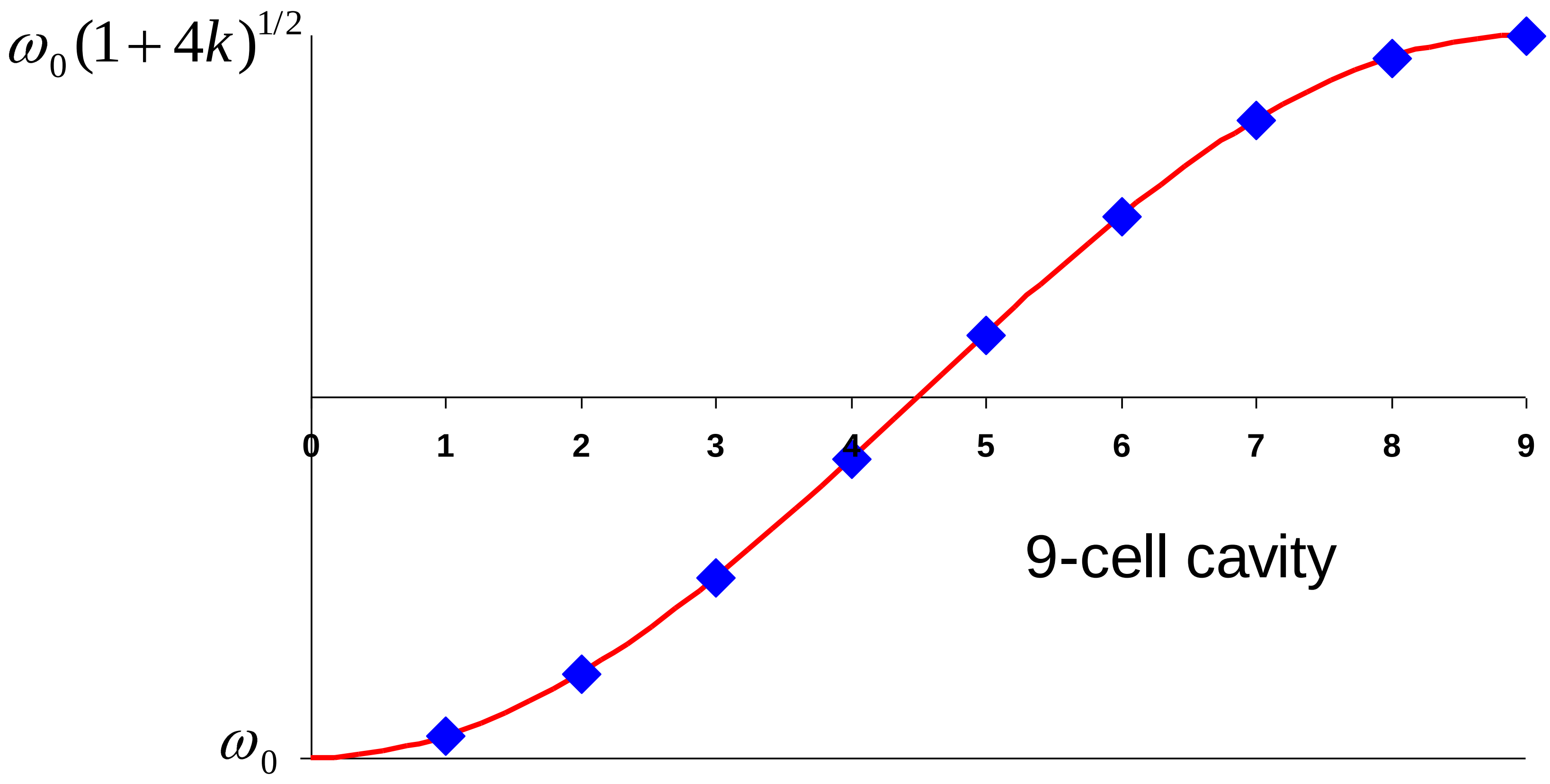

Cell Excitations in Pass-Band Modes

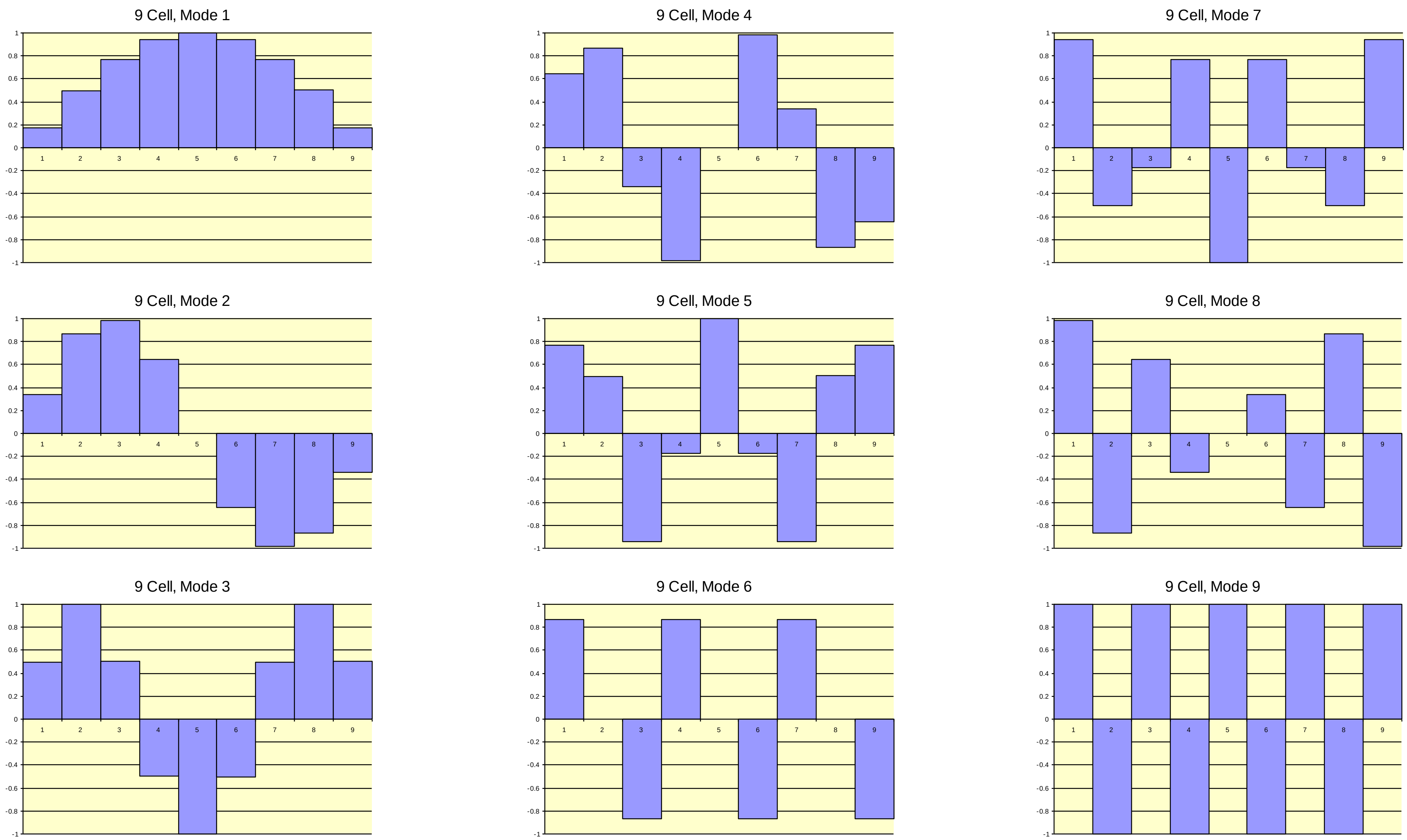

Field Flatness in Multi-Cell Cavities

- Geometrical differences between cells causes a mixing of the eigenmodes
- Sensitivity to mechanical deformation depends on mode spacing

$$\frac{\omega_n - \omega_{n-1}}{\omega_0} = k\left(1-\cos\frac{\pi}{n}\right) = \frac{k}{2}\left(\frac{\pi}{n}\right)^2$$

Low Beta Accelerating Structures – TEM Class Cavities

Classification of Structures

- Two main types of structure geometries
  - TEM class (QW, HW, Spoke)
  - TM class (Elliptical)

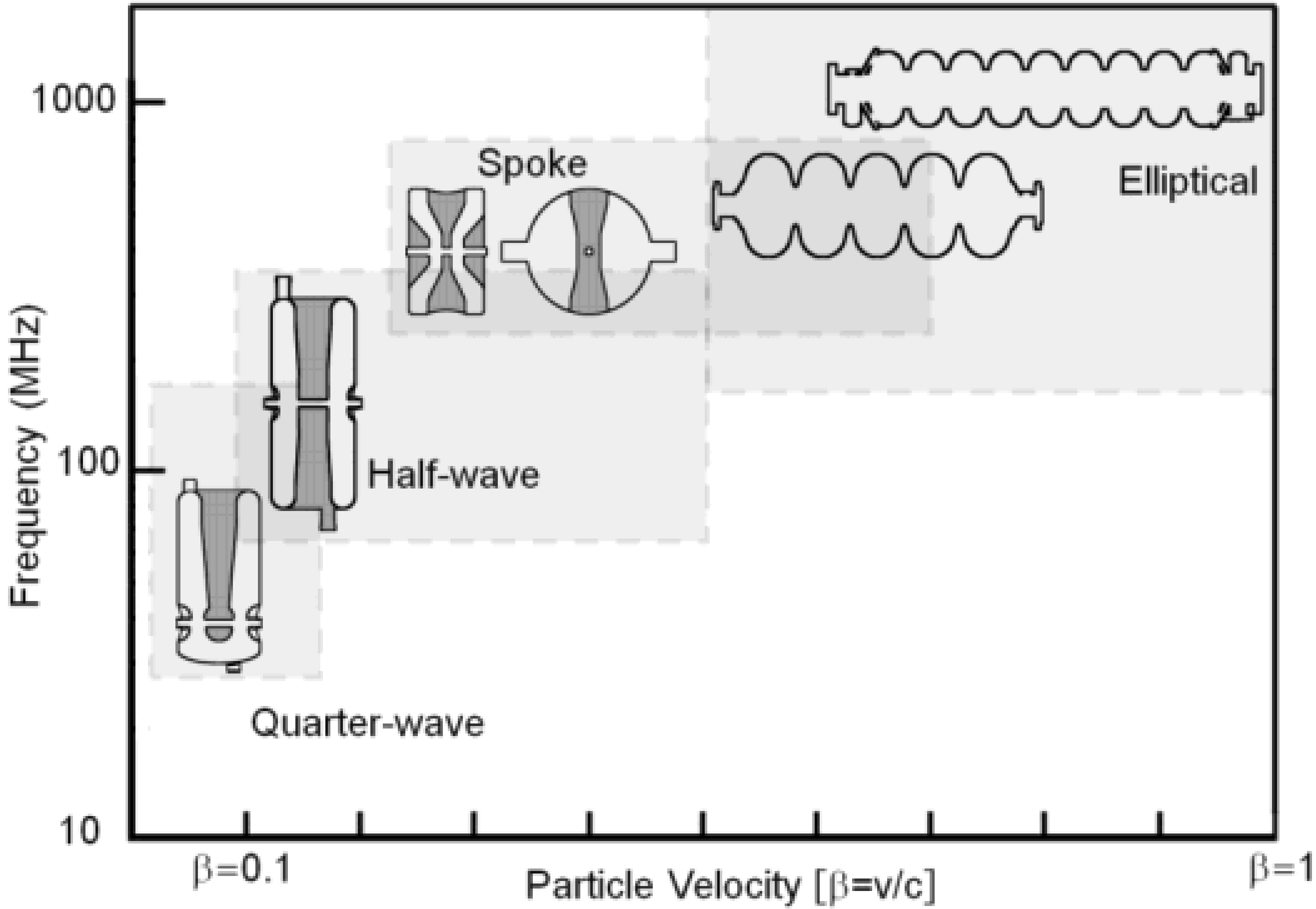

Low β Cavities

- Low β cavities: Cavities that accelerate particles with $\beta < 1$ efficiently
- Increased needs for reduced-beta ($\beta < 1$) SRF cavity especially in CW machines or high duty pulsed machine (duty > 10%)
- Reduced beta Elliptical multi-cell SRF cavity
  - For CW, prototyping by several R&D groups have demonstrated as low as β=0.47
  - For pulsed, SNS β=0.61, 0.81 cavities & ESS
- Elliptical cavity has intrinsic problem as β goes down
  - Mechanical problem, multipacting, low rf efficiency

Applications of Low β Cavities

	High Current	Medium/Low Current
CW	Accelerator driven systems • Waste transmutation • Energy production Beam: p, H^-, d	Production of radioactive ions Nuclear Structure Beam; p to U
Pulsed	Pulsed spallation sources Beam: p, H-	

Technical Issues and Challenges

	High Current	Medium/Low Current
CW	• Beam losses (~ 1 W/m) • Activation • High cw rf power • Higher order modes • Cryogenics losses	• Beam losses (~ 1 W/m) • Activation • High cw rf power • Higher order modes • Cryogenics losses
Pulsed	• Beam losses (~ 1 W/m) • Activation • Higher order modes • High peak rf power • Dynamic Lorentz detuning	

Design Considerations

	High Current	Medium/Low Current
CW	• Cavities with high acceptance • Development of high cw power couplers • Extraction of HOM power • Cavities with high shunt impedance	• Cavities with low sensitivity to vibration • Development of microphonics compensation • Cavities with high shunt impedance • Cavities with large velocity acceptance (few cells) • Cavities with large beam acceptance (low frequency, small frequency transitions)
Pulsed	• Cavities with high acceptance • Development of high peak power couplers • Extraction of HOM power • Development of active compensation of dynamic Lorentz detuning	Note: Large beam acceptance • Large aperture (transverse acceptance) • Low frequency (longitudinal acceptance)

Basic Geometries

- Resonant transmission lines
  - $\lambda/4$
    - ❖ Quarter wave
    - ❖ Split ring
    - ❖ Twin quarter wave
    - ❖ Lollipop
  - $\lambda/2$
    - ❖ Coaxial half wave
    - ❖ Spoke
    - ❖ H-type
- TM type
  - Elliptical
  - Reentrant
- Other
  - Alvarez
  - Slotted iris

Low β Cavities

- Many different shapes and sizes

115 MHz split-ring cavity,

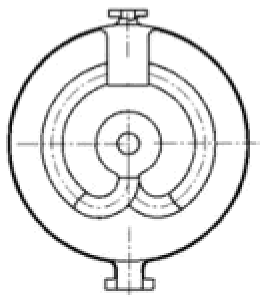

172.5 MHz β = 0.19 "lollipop" cavity

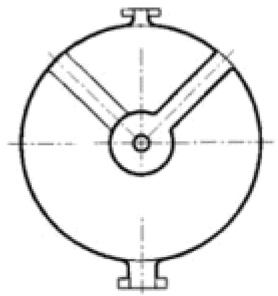

ANL cavities for RIA

QW HW Spoke

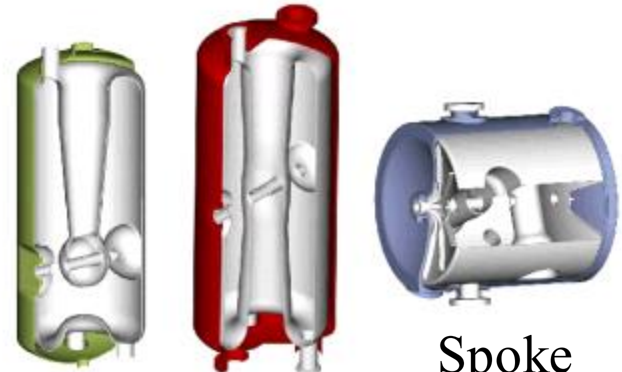

Half-wave cavity

RFQ

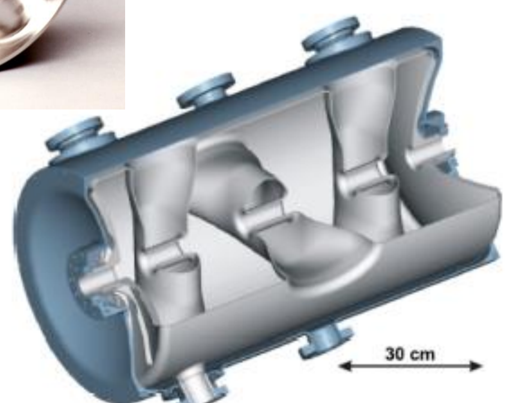

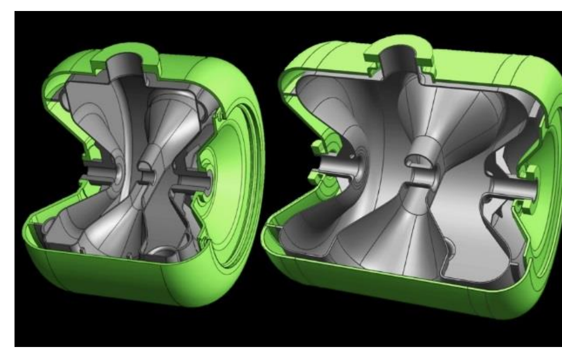

Transit Time Factor

- The transit time factor is the ratio of the acceleration voltage to the (non-physical) voltage a particle with infinite velocity would see

- Energy gain (W): $$\Delta W = q\int_{-\infty}^{+\infty} E(z)\cos(\omega t+\phi)\,dz$$

- Assuming constant velocity

$$\Delta W = q\ \cos\phi\ \ \Delta W_0\ \ T(\beta) \qquad\qquad \Delta W_0 = \Theta \int_{-\infty}^{+\infty} |E(z)|\,dz$$

- Transit time factor: $$\Theta = \frac{\mathrm{Max}\int_{-\infty}^{+\infty} E(z)\cos\left(\dfrac{\omega z}{\beta c}\right)dz}{\int_{-\infty}^{+\infty} |E(z)|\,dz}$$

Velocity Acceptance

- Velocity acceptance

$$T(\beta) = \frac{\int_{-\infty}^{+\infty} E(z)\cos\left(\frac{\omega z}{\beta c}\right) dz}{\text{Max}\int_{-\infty}^{+\infty} E(z)\cos\left(\frac{\omega z}{\beta c}\right) dz}$$

- Lower the velocity of the particle or cavity β
  - Faster the velocity of the particle will change
  - Narrower the velocity range of a particular cavity
  - Smaller the number of cavities of that β
  - More important: Particle achieve design velocity

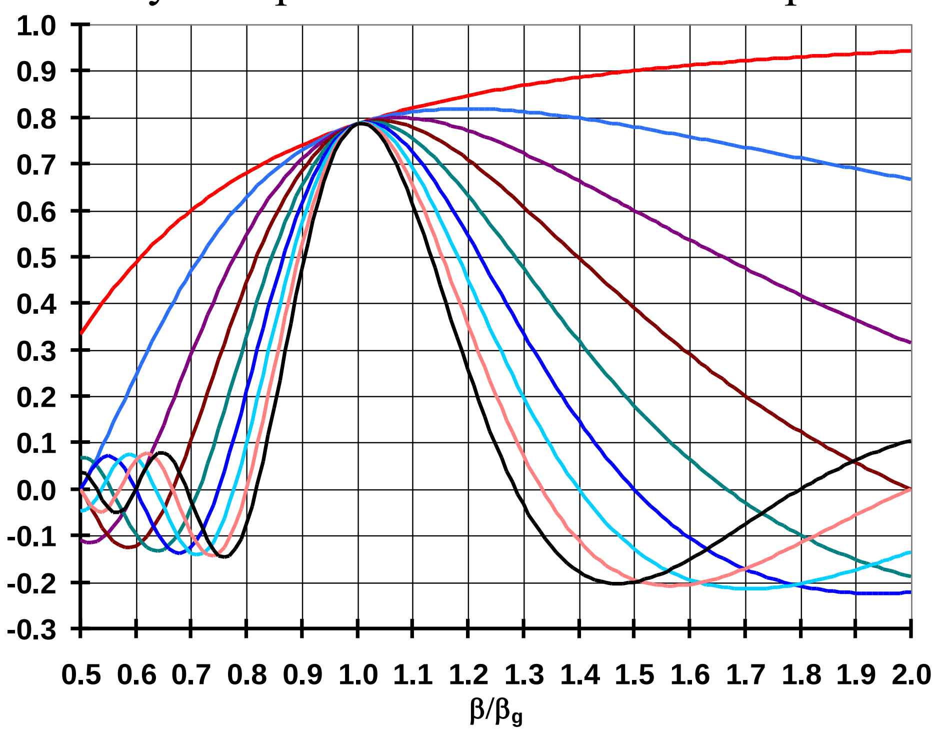

Quarter–Wave Resonator

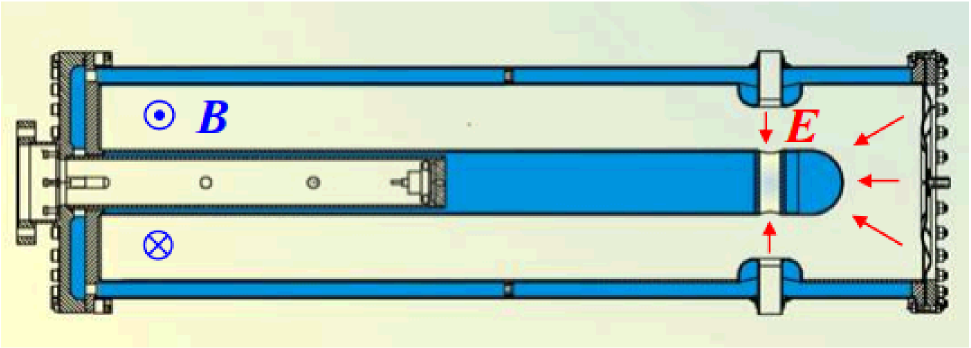

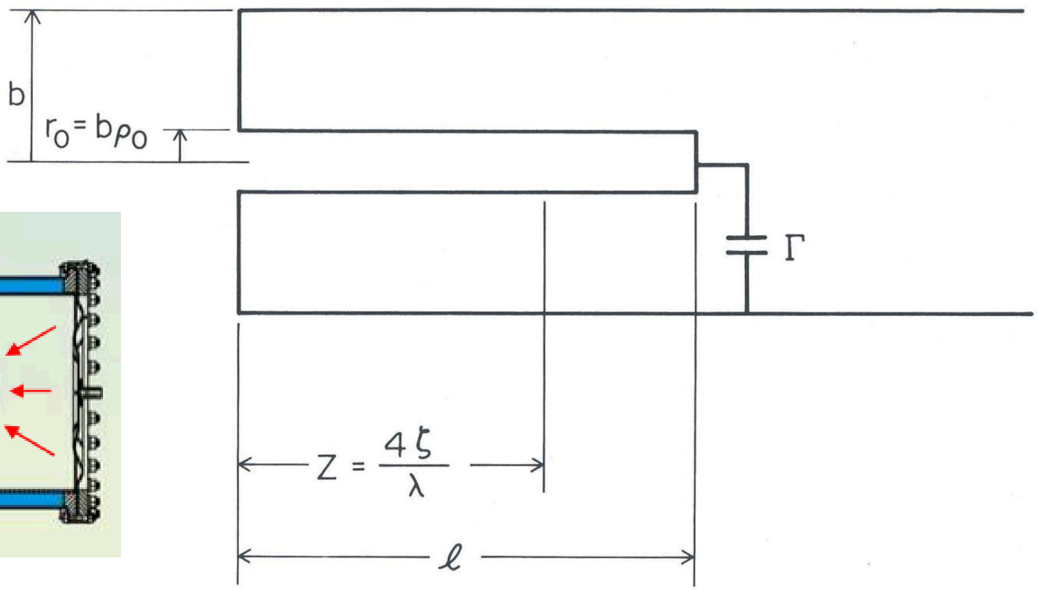

b : radius of outer conductor

$r(z)$: radius of center conductor

r_0 : radius of center conductor at shorting plate

$\rho = r / b$: normalized radius of center conductor

z : distance from shorting plate

$\zeta = 4z / \lambda$: normalized distance from shorting plate

$\eta = \sqrt{\mu_0 / \varepsilon_0} \simeq 377\Omega$: impedance of vacuum

Quarter–Wave Resonator

Capacitively loaded λ/4 transmission line

– Capacitance per unit length:

$$C = \frac{2\pi\varepsilon_0}{\ln(b/r_0)} = \frac{2\pi\varepsilon_0}{\ln(1/\rho_0)}.$$

– Inductance per unit length:

$$L = \frac{\mu_0}{2\pi}\ln\left(\frac{b}{r_0}\right) = \frac{\mu_0}{2\pi}\ln\left(\frac{1}{\rho_0}\right).$$

– Current along the center conductor:

$$I = I_0\cos\left(\frac{2\pi}{\lambda}z\right) = I_0\cos\left(\frac{\pi}{2}\zeta\right).$$

–Voltage along the center conductor:

$$V = V_0\sin\left(\frac{2\pi}{\lambda}z\right) = V_0\sin\left(\frac{\pi}{2}\zeta\right).$$

– Transmission line impedance:

$$Z_0 = \frac{V_0}{I_0} = \frac{\eta}{2\pi}\ln\left(\frac{1}{\rho_0}\right).$$

– Loading capacitance:

$$\Gamma = \lambda\varepsilon_0\frac{\operatorname{cotan}\left(\frac{2\pi}{\lambda}z\right)}{\ln(b/r_0)} = \lambda\varepsilon_0\frac{\operatorname{cotan}\left(\frac{\pi}{2}\zeta\right)}{\ln(1/\rho_0)}.$$

The transmission line can be shorter than λ/4 and still resonate at the right frequency if it is terminated by the appropriate loading capacitance Γ.

$$l = \frac{\lambda}{2\pi}\mathrm{Arctan}\left[\frac{\lambda\varepsilon}{\Gamma\ln(1/\rho_0)}\right]$$

Quarter–Wave Resonator

Cavity parameters:

– Peak magnetic field

$$\frac{V_p}{b} = \begin{Bmatrix} \eta & H \\ c & B \\ 300 & B \end{Bmatrix} \rho_0 \ln\left(\frac{1}{\rho_0}\right) \sin\left(\frac{\pi}{2}\zeta\right) \quad \begin{Bmatrix} \text{m, A/m} \\ \text{m, T} \\ \text{cm, G} \end{Bmatrix}$$

V_p: Voltage across loading capacitance

– Power dissipation

$$P = V_p^2 \frac{\pi}{8} \frac{R_s}{\eta^2} \frac{\lambda}{b} \frac{1+1/\rho_0}{\ln^2 \rho_0} \frac{\zeta + \frac{1}{\pi}\sin \pi\zeta}{\sin^2 \frac{\pi}{2}\zeta} \propto \frac{R_s}{\eta^2} E^2 \beta \lambda^2$$

Ignore losses in the end plate

– Stored energy

$$U = V_p^2 \frac{\pi\varepsilon_0}{8} \lambda \frac{1}{\ln(1/\rho_0)} \frac{\zeta + \frac{1}{\pi}\sin \pi\zeta}{\sin^2 \frac{\pi}{2}\zeta} \propto \varepsilon_0 E^2 \beta^2 \lambda^3$$

– Geometrical factor

$$G = QR_s = 2\pi\,\eta \frac{b}{\lambda} \frac{\ln(1/\rho_0)}{1+1/\rho_0} \propto \eta\,\beta$$

– Shunt impedance

$$R_{sh} = \frac{\eta^2}{R_s} \frac{32}{\pi} \frac{b}{\lambda} \frac{\ln^2 \rho_0}{1+1/\rho_0} \frac{\sin^2 \frac{\pi}{2}\zeta}{\zeta + \frac{1}{\pi}\sin \pi\zeta}$$

$$R_{sh}\, R_s \propto \eta^2\, \beta$$

– R/Q

$$\frac{R_{sh}}{Q} = \frac{16}{\pi^2}\eta \ln(1/\rho_0) \frac{\sin^2 \frac{\pi}{2}\zeta}{\zeta + \frac{1}{\pi}\sin \pi\zeta} \propto \eta$$

Half–Wave Resonator

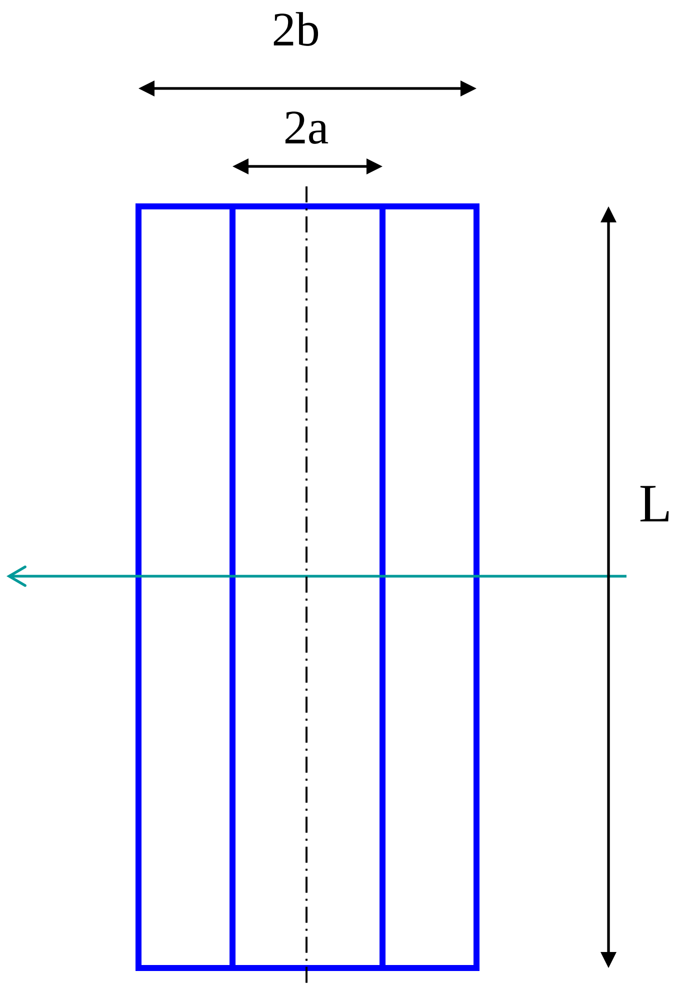

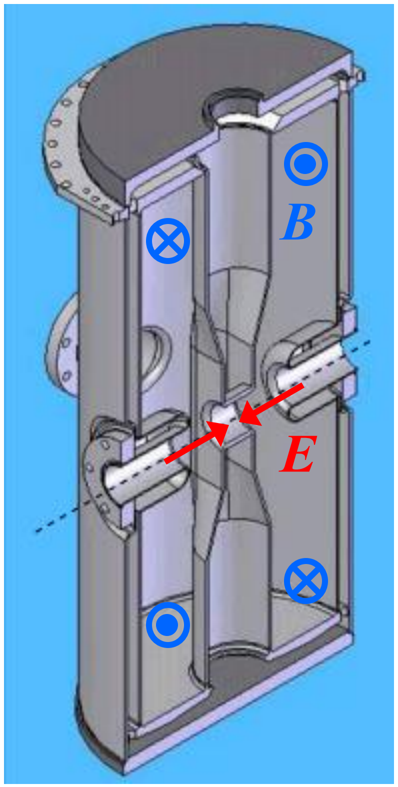

The first 355 MHz SC HWR ANL - β=0.12

Half–Wave Resonator

– Capacitance per unit length

$$C = \frac{2\pi\varepsilon_0}{\ln\left(\frac{b}{a}\right)} = \frac{2\pi\varepsilon_0}{\ln\left(\frac{1}{\rho_0}\right)}$$

– Inductance per unit length

$$L = \frac{\mu_0}{2\pi}\ln\left(\frac{b}{r_0}\right) = \frac{\mu_0}{2\pi}\ln\left(\frac{1}{\rho_0}\right)$$

– Center conductor voltage

$$V(z) = V_0 \cos\left(\frac{2\pi}{\lambda} z\right)$$

– Center conductor current

$$I(z) = I_0 \sin\left(\frac{2\pi}{\lambda} z\right)$$

– Line impedance

$$Z_0 = \frac{V_0}{I_0} = \frac{\eta}{2\pi}\ln\left(\frac{1}{\rho_0}\right)$$

Half–Wave Resonator

Cavity parameters:

– Peak magnetic field

$$\frac{V_p}{b} = \begin{Bmatrix} \eta & H \\ c & B \\ 300 & B \end{Bmatrix} \rho_0 \ln\left(\frac{1}{\rho_0}\right) \qquad \begin{Bmatrix} \text{m, A/m} \\ \text{m, T} \\ \text{cm, G} \end{Bmatrix}$$

V_p: Voltage across loading capacitance

– Power dissipation

$$P = V_p^2 \frac{\pi}{4} \frac{R_s}{\eta^2} \frac{\lambda}{b} \frac{1+1/\rho_0}{\ln^2 \rho_0} \quad \propto \frac{R_s}{\eta^2} E^2 \beta \lambda^2$$

Ignore losses in the end plates

– Stored energy

$$U = V_p^2 \frac{\pi\varepsilon_0}{4} \lambda \frac{1}{\ln(1/\rho_0)} \quad \propto \varepsilon_0 E^2 \beta^2 \lambda^3$$

– Geometrical factor

$$G = QR_s = 2\pi\,\eta \frac{b}{\lambda} \frac{\ln(1/\rho_0)}{1+1/\rho_0} \propto \eta\,\beta$$

– Shunt impedance

$$R_{sh} = \frac{\eta^2}{R_s} \frac{16}{\pi} \frac{b}{\lambda} \frac{\ln^2 \rho_0}{1+1/\rho_0}$$

$$R_{sh}\, R_s \propto \eta^2\, \beta$$

– R/Q

$$\frac{R_{sh}}{Q} = \frac{8}{\pi^2} \eta \ln(1/\rho_0) \quad \propto \eta$$

Spoke Resonators

There have been extensive efforts for design optimization especially to reduce the ratios of

E_p/E_{acc} and B_p/E_{acc}

- Controlling A/B (E_p/E_{acc}) and C/D (B_p/E_{acc}) → Shape optimization
- Flat contacting surface at spoke base will also help in minimization of B_p/E_{acc}
- For these cavities:
  - Calculations agree well → E_p/E_{acc}~3, B_p/E_{acc}~(7~8) mT/(MV/m)
  - Though it is tricky to obtain precise surface field information from the 3D simulation

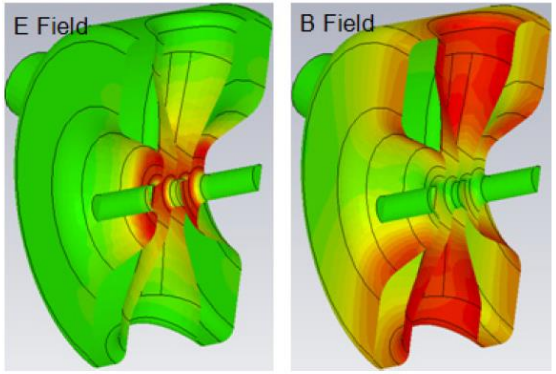

325 MHz, β=0.17 (FNAL)

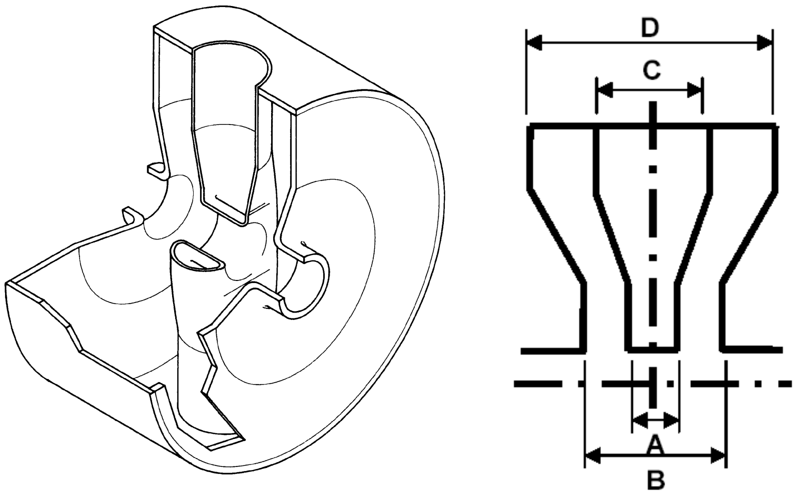

Spoke Resonators

- $E_p/E_a \sim 3.3$, independent of β
- $B/E_a \sim 8$ mT/(MV/m), independent of β

Surface electric field

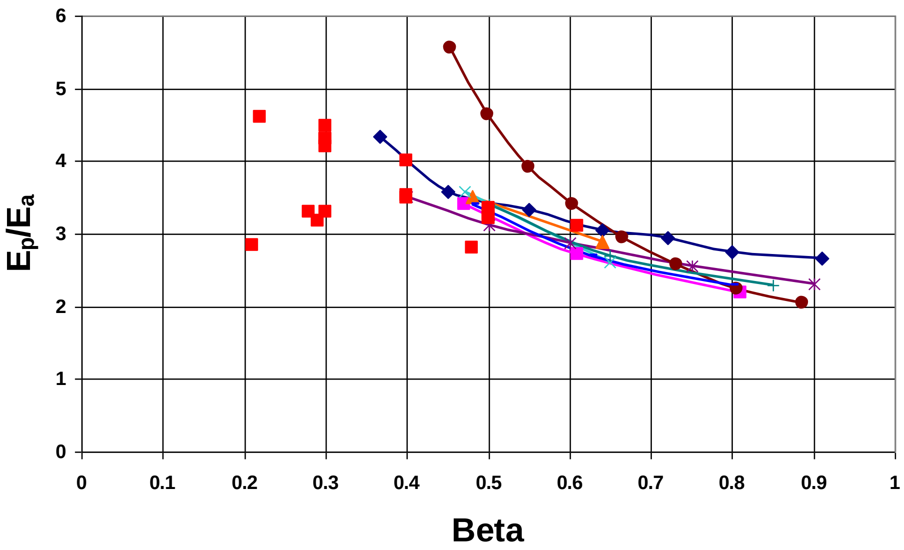

Surface magnetic field

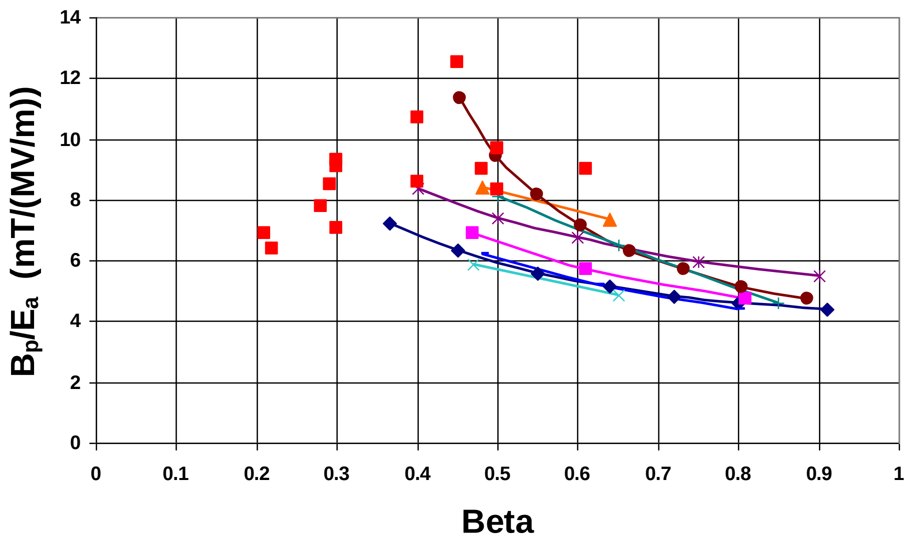

Lines: Elliptical

Squares: Spoke

Spoke Resonators

- $QR_s \sim 200\,\beta\ [\Omega]$
- $R_{sh}/Q \sim 205\ [\Omega]$, independent of β

Geometrical factor

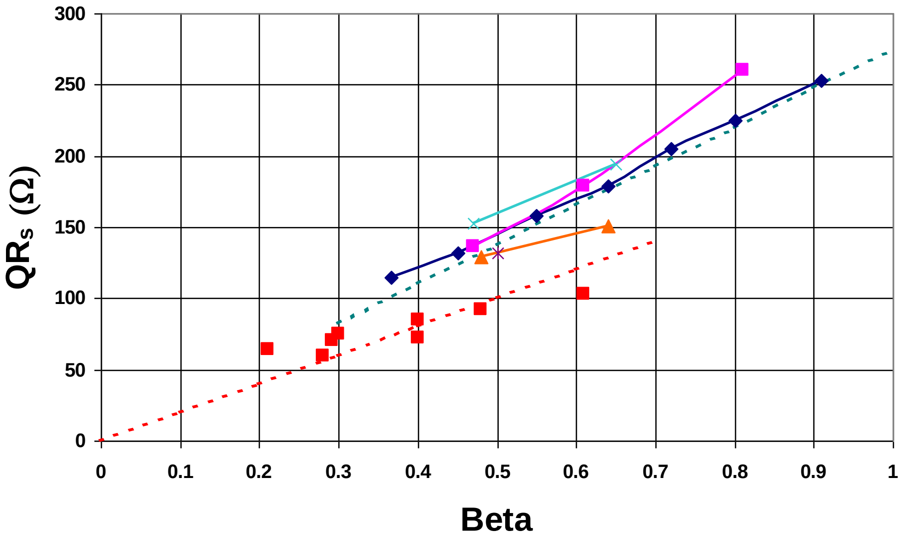

R_{sh}/Q

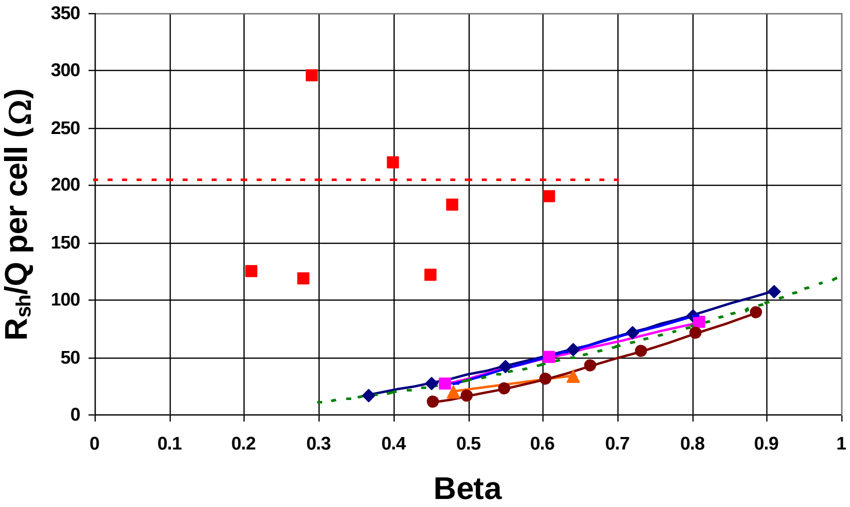

Lines: Elliptical

Squares: Spoke

Spoke Resonators

- $R_{sh}\, R_s \;\sim\; 40000\, \beta \quad [\Omega^2]$
- $U/E^2 \sim 200\, \beta^2 \quad [\mathrm{mJ}]$

$R_{sh}\, R_s$

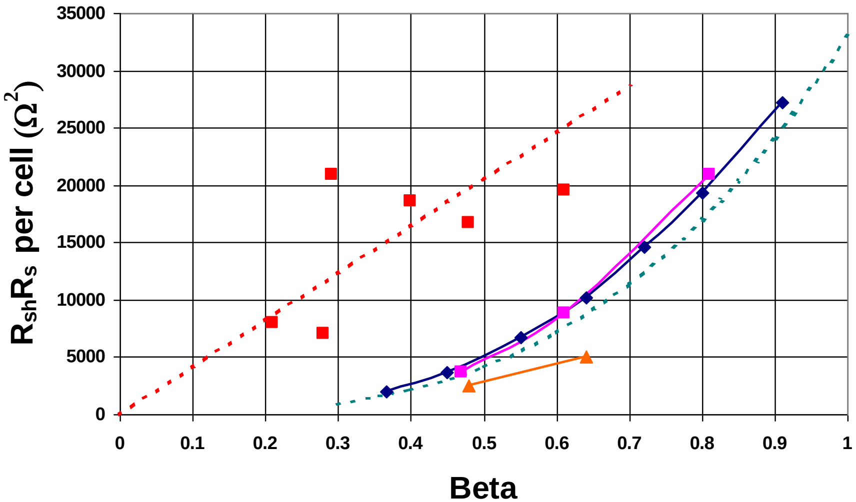

U/E^2

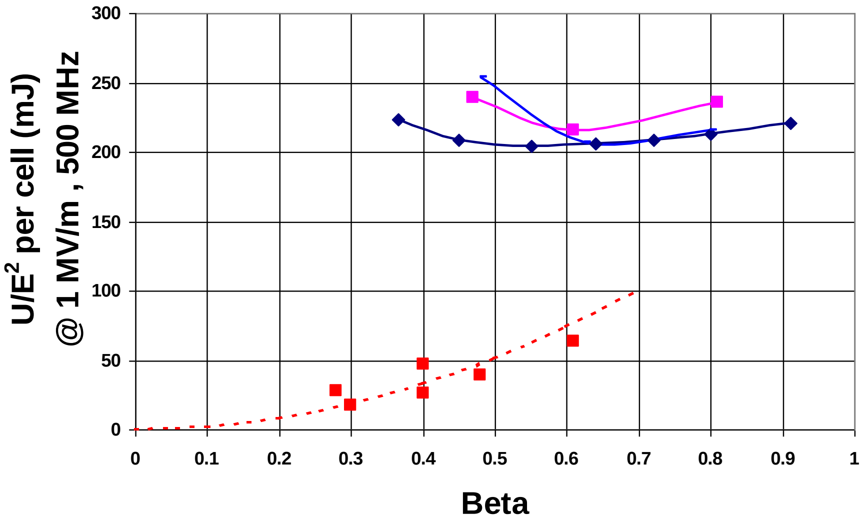

Lines: Elliptical Squares: Spoke

Features of Spoke Cavities

- **Small Size**
  – **About half of TM cavity of same frequency**

- Allows low frequency at reasonable size
  – Possibility of 4.2 K operation
  – High longitudinal acceptance

- Fewer number of cells
  – Wider velocity acceptance

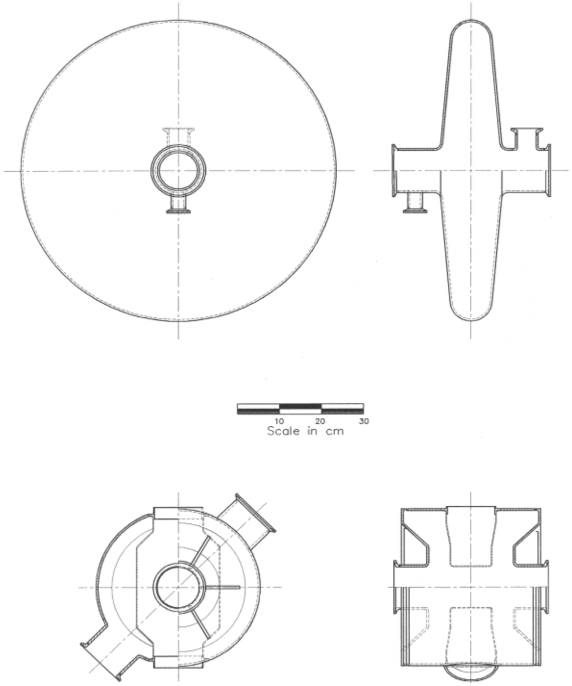

350 MHz, β= 0.45

Deflecting / Crabbing Cavities

Deflecting Cavities

- Complete bunch is deflected with the transverse kick applied at the center of the bunch

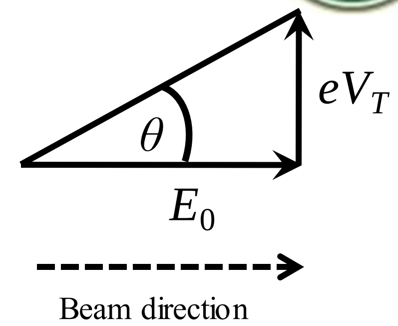

$$\theta = \arctan\left[\frac{eV_t}{E_0}\right] \sim \frac{eV_t}{E_0}$$

$$\mathrm{V}_t = E_0\,[eV]\,\theta\,[rad]$$

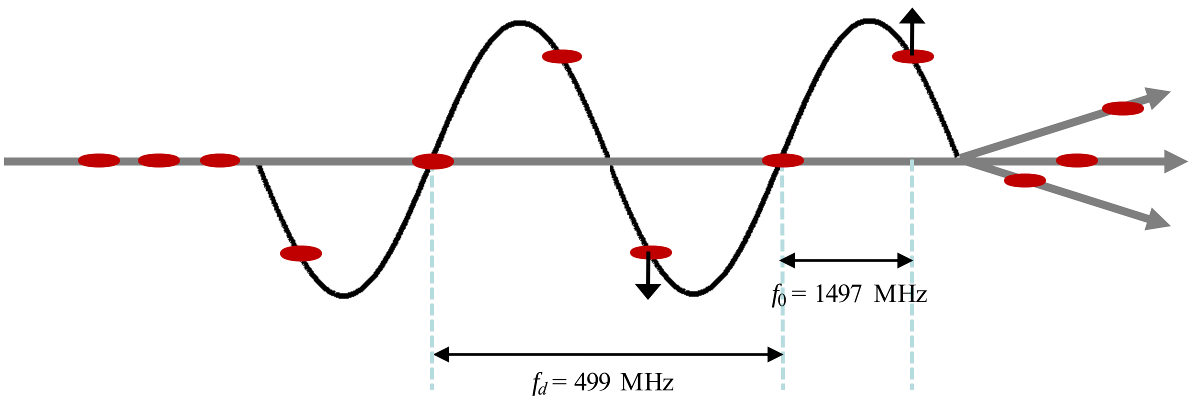

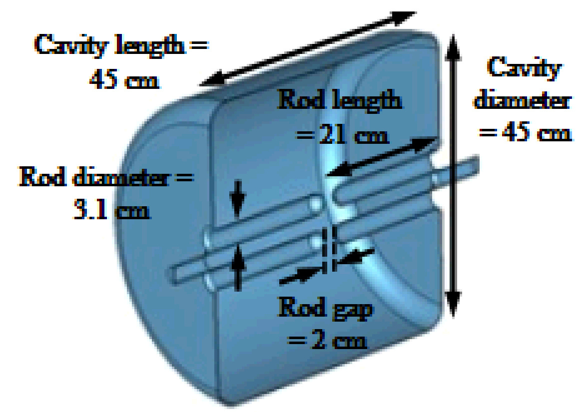

- RF frequency (f_d) = 499 MHz
- Beam energy (E) = 11.023 GeV
- Deflecting angle (θ)
- Transverse voltage (V_t)

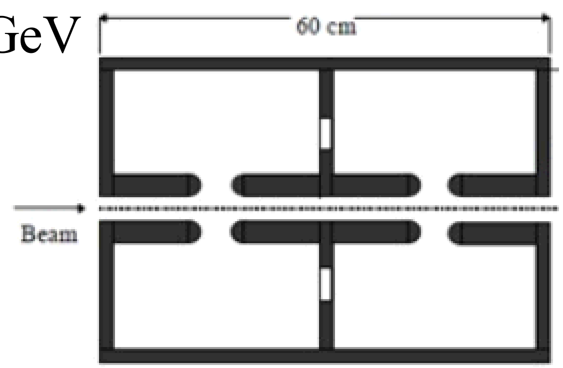

Crabbing Cavities

- Luminosity with no crabbing system:

$$\mathcal{L} = \frac{N_1 N_2 f_c N_b}{4\pi\sigma_x\sigma_y} F_c = \frac{N_1 N_2 f_c N_b}{4\pi\sigma_x\sigma_y} \frac{1}{\sqrt{1+\left(\frac{\sigma_z\theta_c}{2\sigma_x}\right)^2}}$$

- Luminosity with crabbing system:
  - For head-on collision

$$\mathcal{L} = \frac{N_1 N_2 f_c N_b}{4\pi\sigma_x\sigma_y}$$

- Transverse voltage

$$V_t = \frac{cE_0 \tan(\theta_c/2)}{\omega\sqrt{\beta_{crab}\beta^*}\sin\left(\psi^x_{cc\to ip}\right)}$$

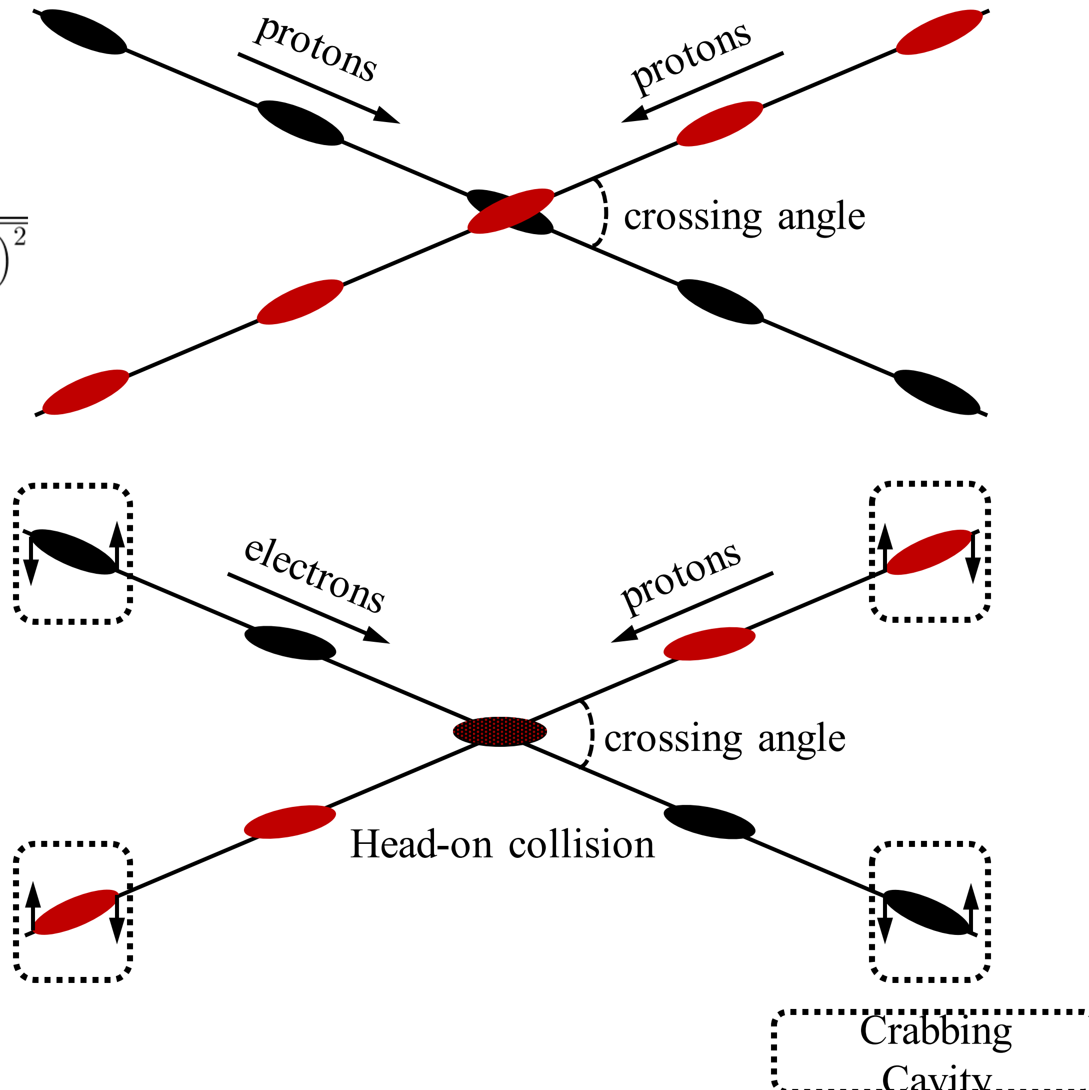

Deflecting/Crabbing Concept

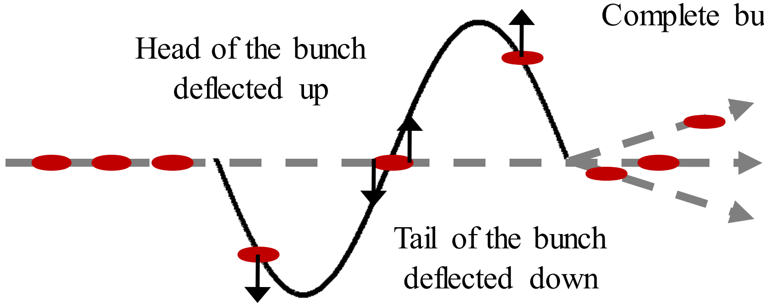

- Both deflecting and crabbing resonant cavities are required to generate a transverse momentum
- Can be produced by either or by both transverse electric (E_t) and magnetic (B_t) fields
- Lorentz force: $\vec{p}_t = \int_{-\infty}^{\infty} \vec{F}_t \, \mathrm{d}t = \frac{q}{v} \int_{-\infty}^{+\infty} \left[\vec{E}_t + j(\vec{v} \times \vec{B}_t) \right] \mathrm{d}z$
- Types of designs:
  - TM-type designs → Main contribution from B_t
  - TE-type designs → Main contribution from E_t
  - TEM-type designs → Contribution from both E_t and B_t

Panofsky–Wenzel Theorem

- For particles moving virtually at v=c, the integrated transverse force (kick) can be determined from the transverse variation of the integrated longitudinal force

$$j\frac{\omega}{c}\vec{F}_t = \nabla_t \vec{F}_z$$

- Transverse momentum is related to the gradient of the longitudinal electric field along the beam axis

$$\vec{p}_t = -i\frac{q}{\omega}\int_{-\infty}^{+\infty}\vec{\nabla}_t E_z \,\mathrm{d}z$$

$$p_t = -i\frac{q}{\omega}\lim_{r_0\to 0}\frac{1}{r_0}\int_{-\infty}^{+\infty}[E_z(r_0, z) - E_z(0, z)]\,\mathrm{d}z$$

- According to the theorem:
  - In a pure TE mode the contribution to the deflection from the magnetic field is completely cancelled by the contribution from the electric field

W.K.H. Panofsky, W.A. Wenzel: "Some Considerations Concerning the Transverse Deflection of Charged Particles in Radio-Frequency Fields", RSI **27**, 1957]

Deflecting/Crabbing Cavities

KEK TM_{110} crabbing cavity

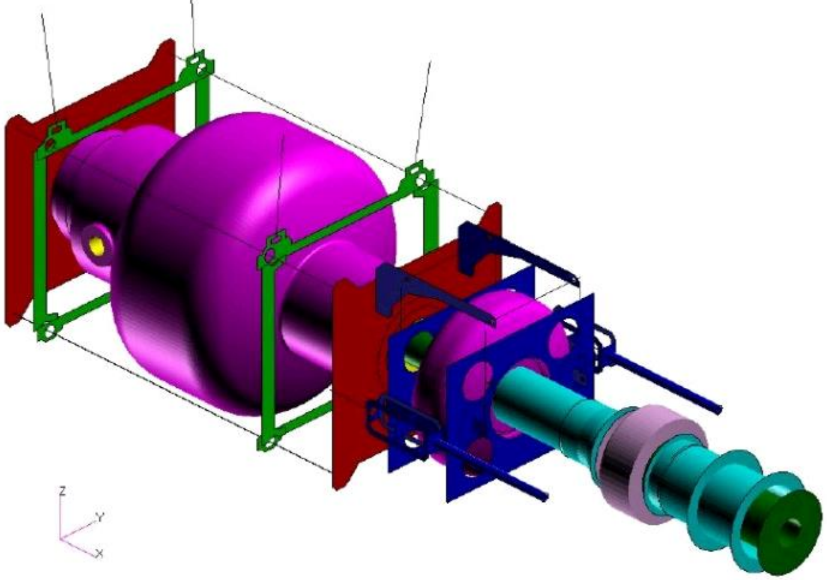

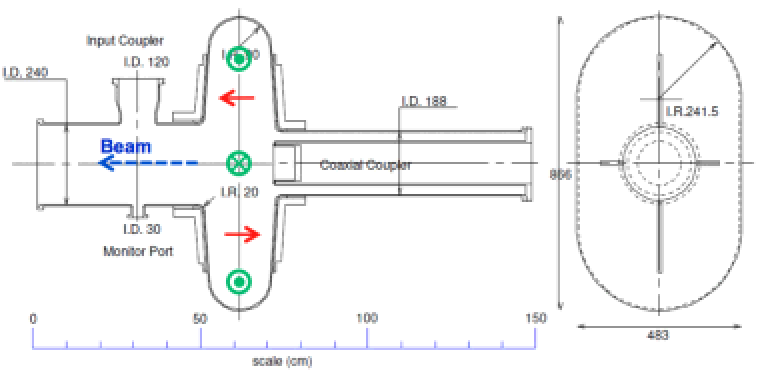

Superconducting 4-rod cavity

BNL double quarter-wave cavity

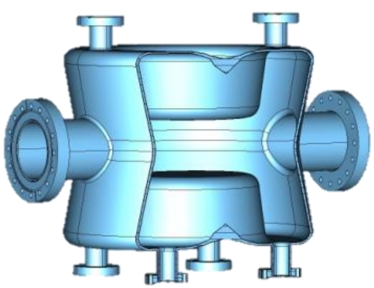

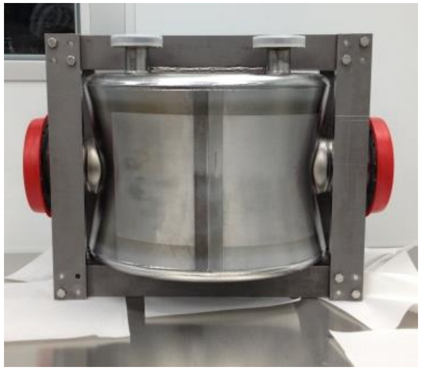

Deflecting/Crabbing Cavities

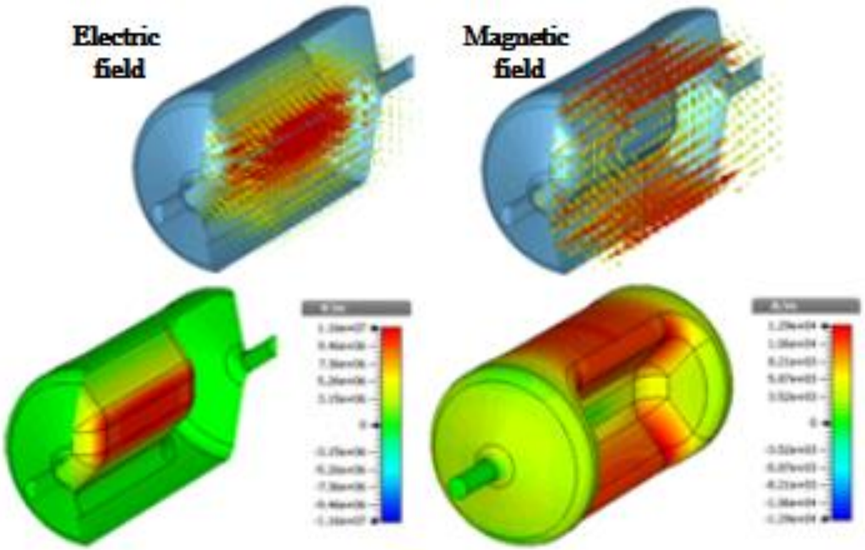

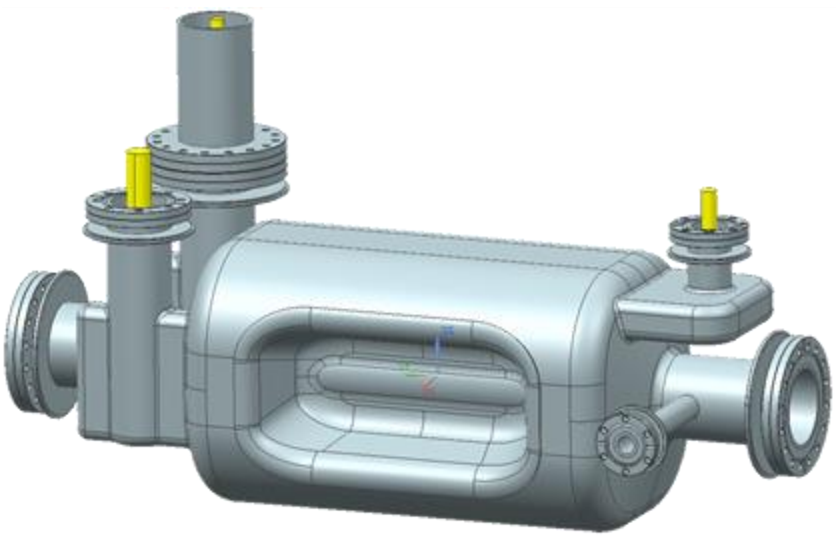

LHC High Luminosity Upgrade

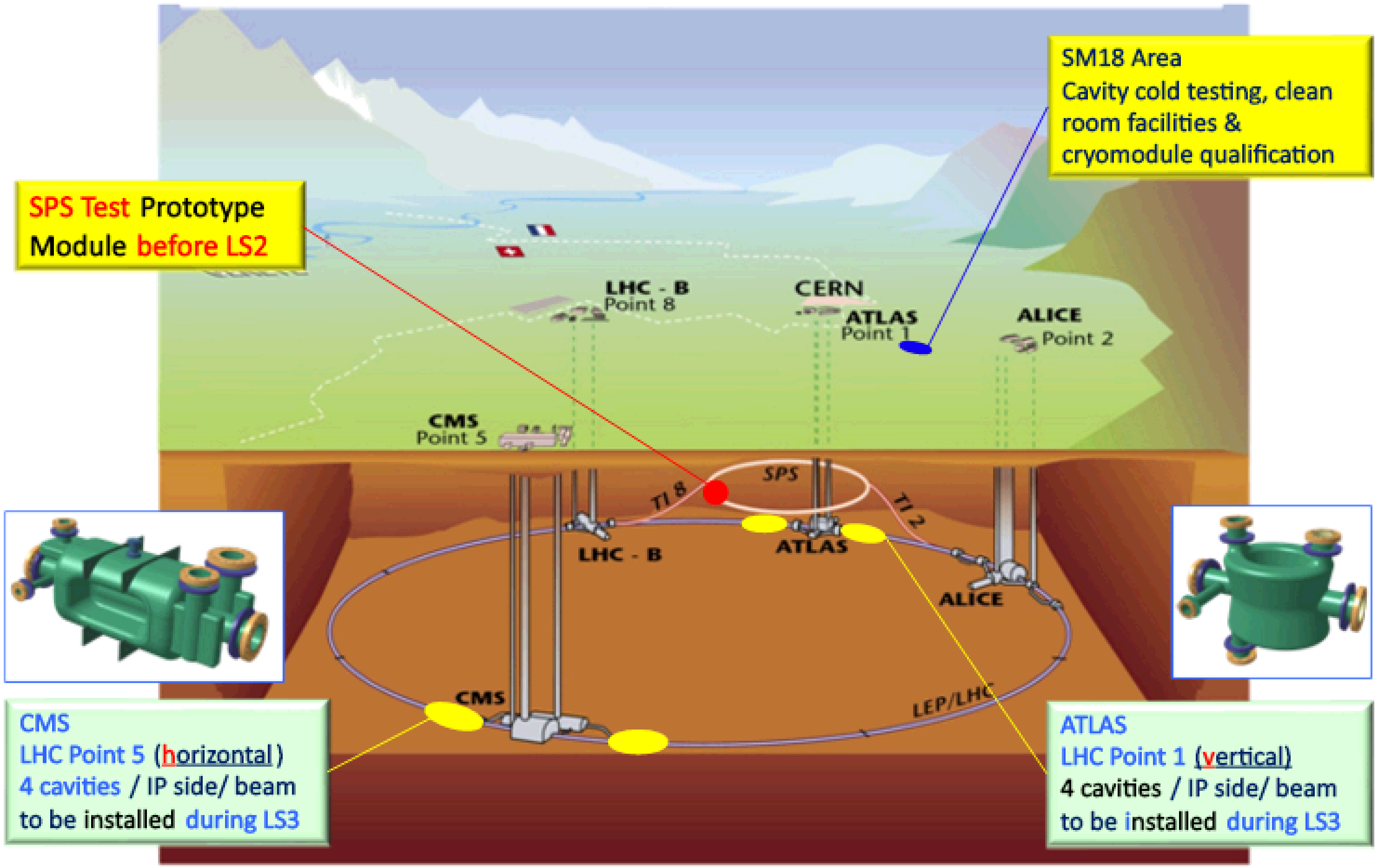

Cavity Limitations

Cavity Performance

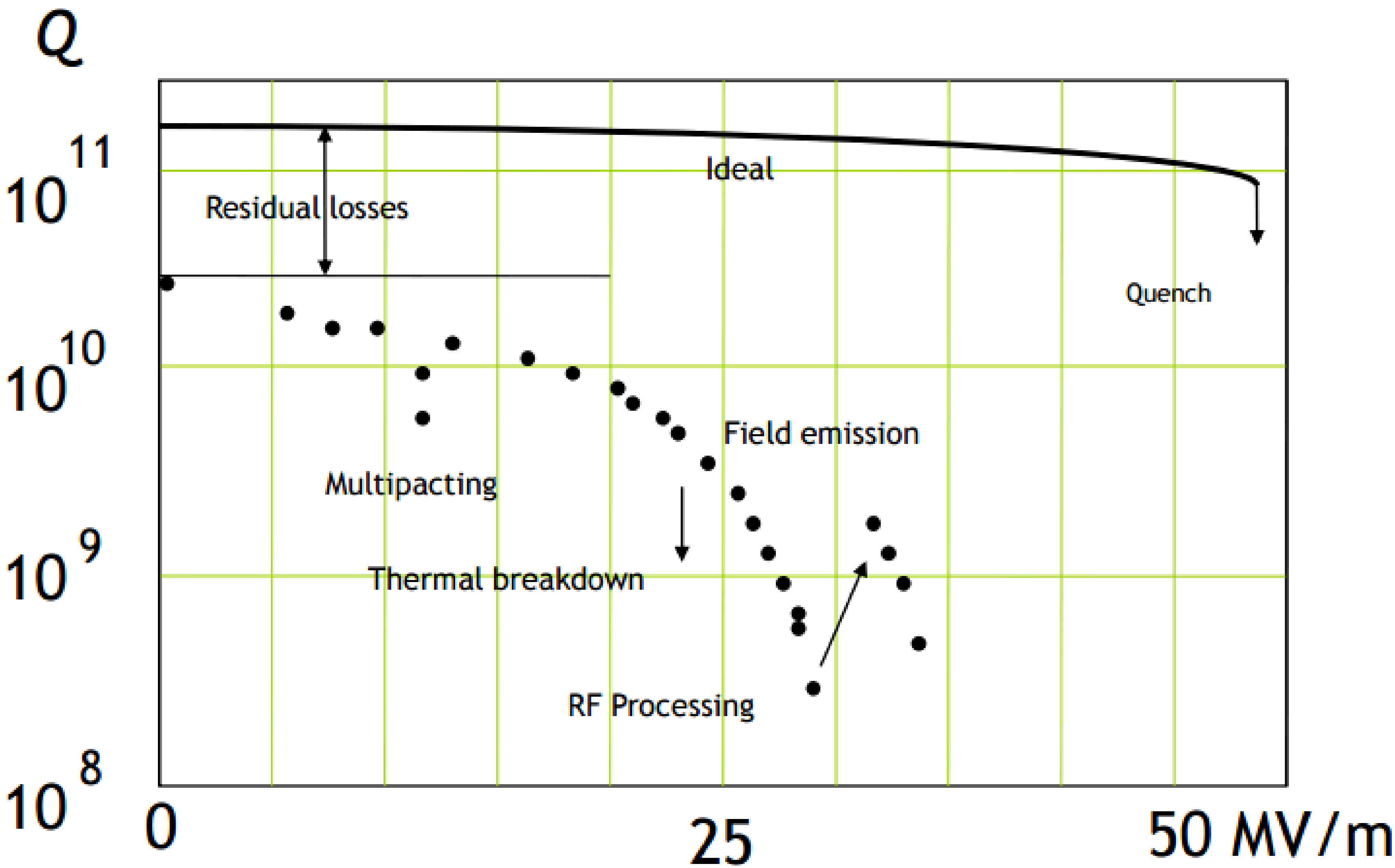

Multipacting

- Multipacting condition – A large amount of secondary electrons are emitted from the cavity surface by the incident primary electrons

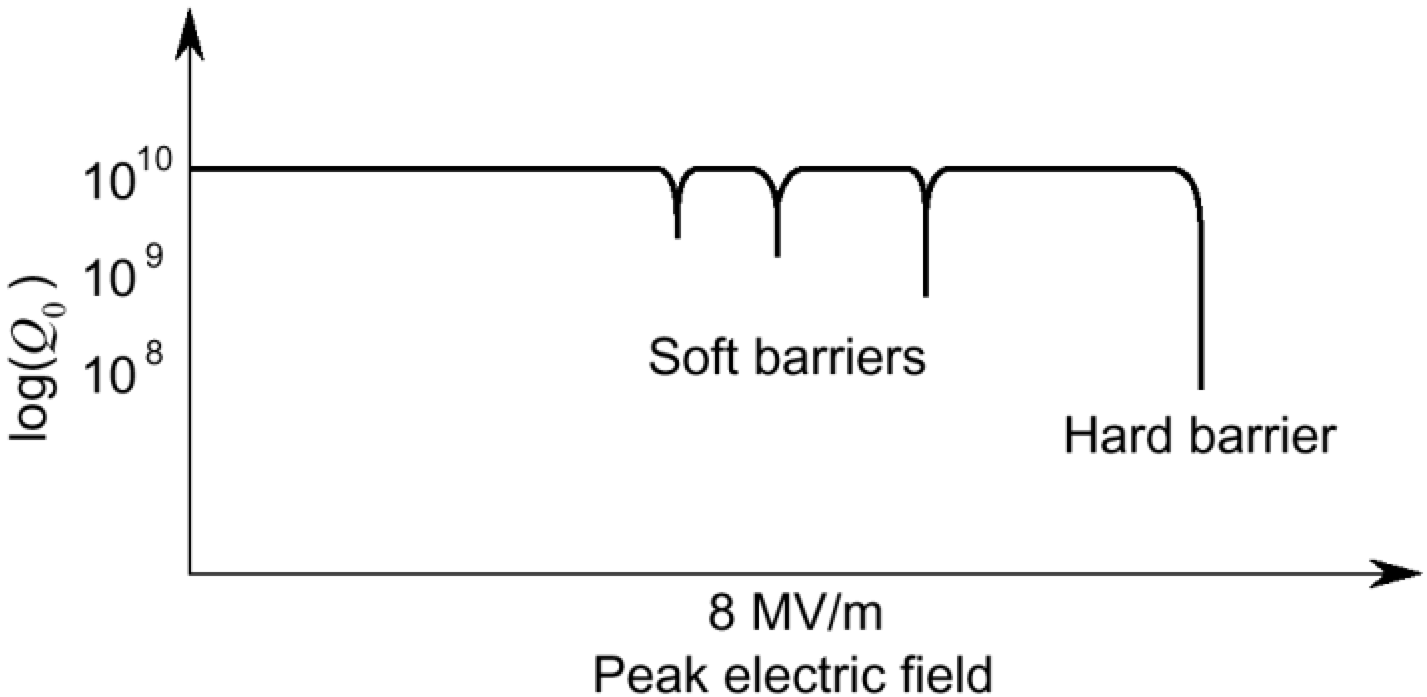

Multipacting

- Resonant condition
  – The secondary electrons have localized and sustainable resonant trajectories with the cavity rf fields
  – Impact energies corresponds to a secondary emission yield (SEY) greater than one

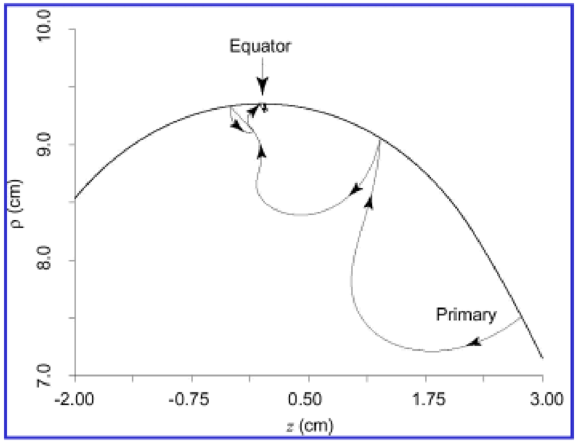

For Nb: $E_I > 150\,eV$ $\quad E_{II} < 2000\,eV$

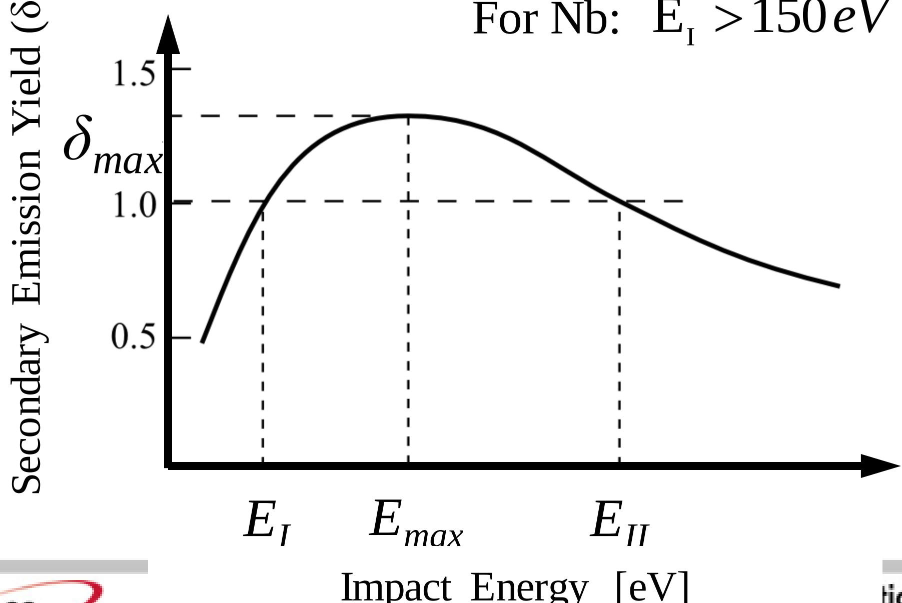

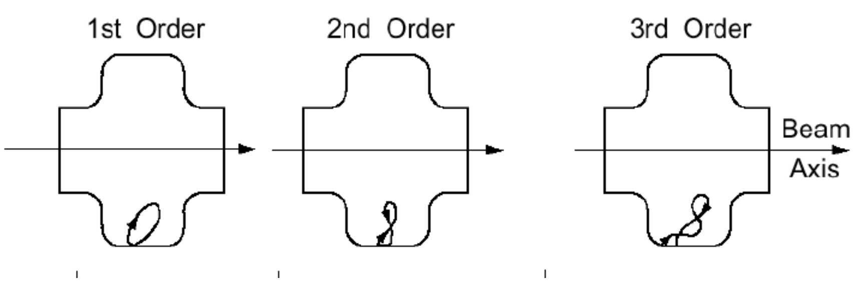

Field Emission

- Characterized by exponential decay in Q_0
- Exponential increase of losses due to acceleration of electron field emission
- With the increasing rf field the field emitters generate an electron current leading to excessive heating and x-rays produced by bremsstrahlung
- It is a general difficulty in accelerating structures, but does not present an ultimate fundamental limit to the maximum surface electric field
- Main cause of FE is particulate contamination

Temperature map shows line heating along the longitude at the location of the emitter

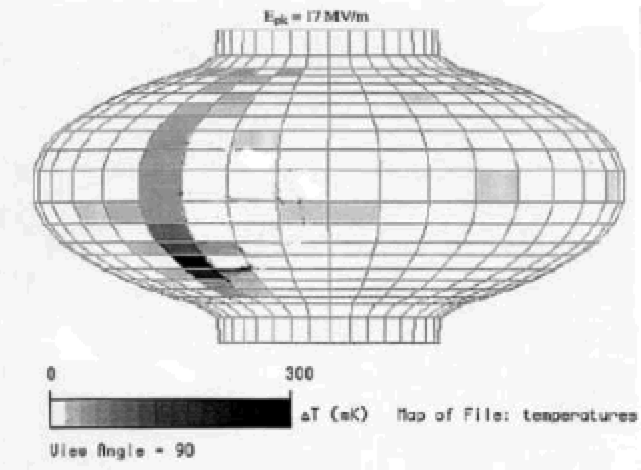

Field Emission

- Fowler and Nordheim (FN) showed that when the work function barrier at the metal surface is lowered by an applied surface electric field, electrons can tunnel through

- Electrostatic potential of the metal-vacuum interface

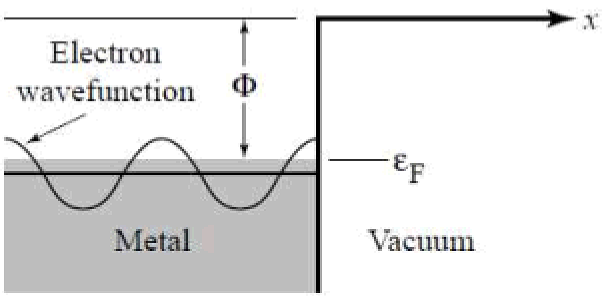

No electric field applied

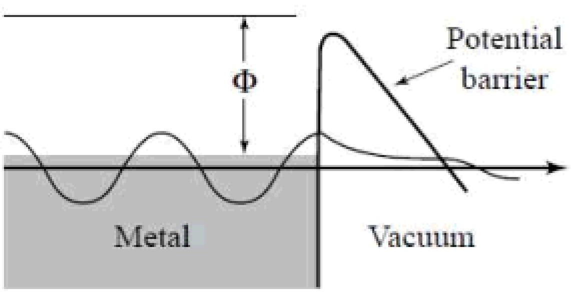

Electric field applied

- Tunneling current density $$J = \frac{1.54\times10^{-6}E^2}{\Phi}\exp\left(-\frac{6.83\times10^{9}\Phi^{3/2}}{E}\right)$$

J : Current density (A/m^2)

E : Electric field (MV/m)

Φ : Work function (eV)

Field Emission

- Modified Fowler Nordheim equation for rf fields

$$J = k\frac{1.54\times10^{-6}(\beta E)^{5/2}}{\Phi}\exp\left(-\frac{6.83\times10^{9}\Phi^{3/2}}{\beta E}\right)$$

β : Enhancement factor (10s to 100s)

k : Effective emitting surface

- Field emitters

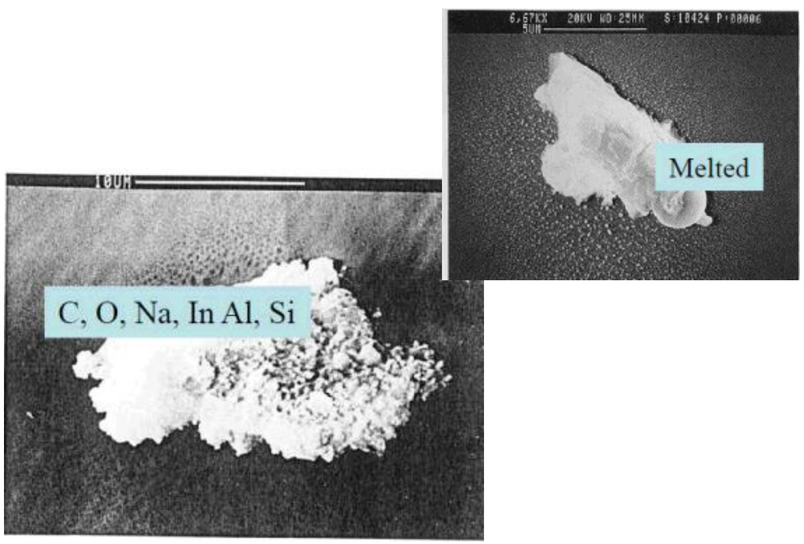

- FE can be prevented by proper surface preparation and contamination control
- Possible to reduce if not completely eliminate FE using CW RF processing, High-power Pulsed Processing (HPP) and/or Helium processing

Ponderomotive Effects

- Ponderomotive effects: changes in frequency caused by the electromagnetic field (radiation pressure)
  - Static Lorentz detuning (CW operation)
  - Dynamic Lorentz detuning (pulsed operation)
- Microphonics: changes in frequency caused by connections to the external world
  - Vibrations
  - Pressure fluctuations
- Note: The two are not completely independent. When phase and amplitude feedbacks are active, the ponderomotive effects can change the response to external disturbances

Lorentz Force Detuning

- Electromagnetic fields in a cavity exert Lorentz forces on the cavity wall. The force per unit area (radiation pressure) is given by

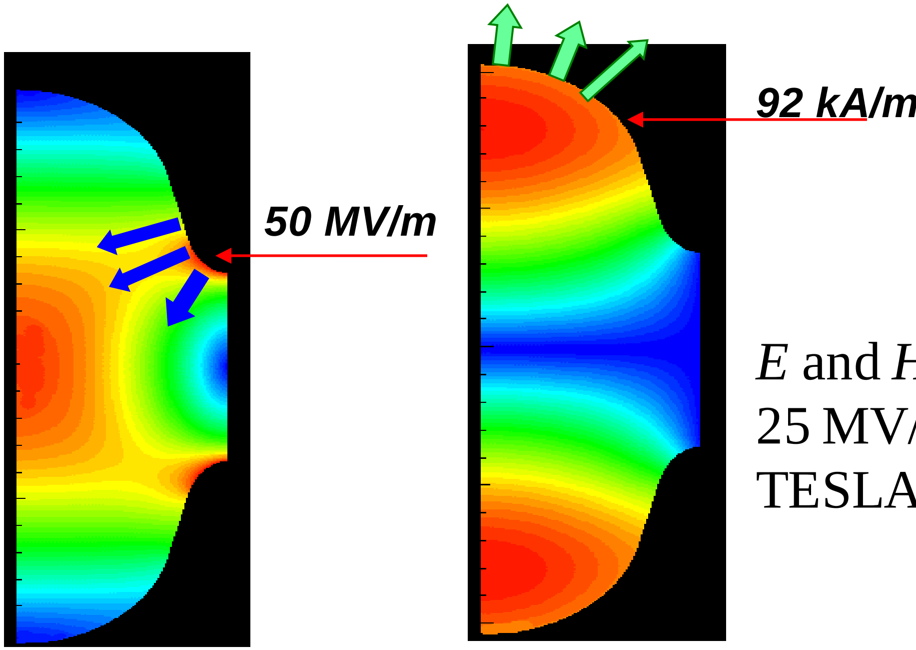

$$P = \frac{\mu_0 H_s^2 - \varepsilon_0 E_s^2}{4}$$

E and H at E_{acc} = 25 MV/m in TESLA inner-cup

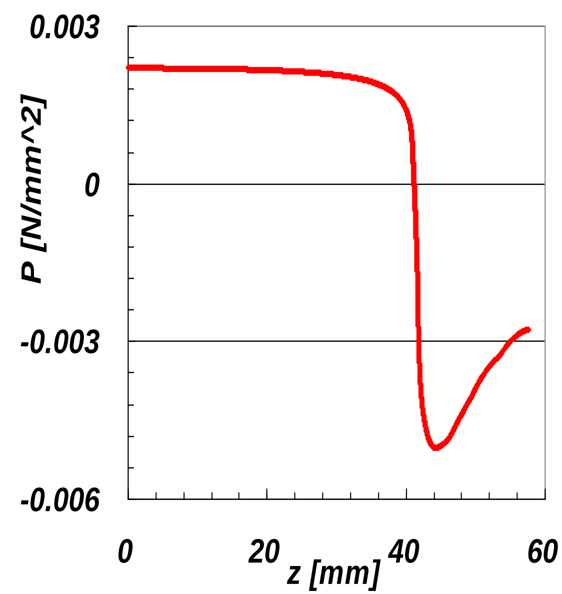

- Residual deformation of the cavity shape shifts the resonant frequency

$$\frac{\Delta f_L}{f} \approx \frac{1}{4U} \int_{\Delta V} \left(\mu_0 H^2 - \varepsilon_0 E^2\right) dv \qquad \Delta f_{L,stat} = -K_L \cdot E_{acc}^2$$

k_{L} – Lorentz coefficient

Thermal Breakdown

- Localized heating

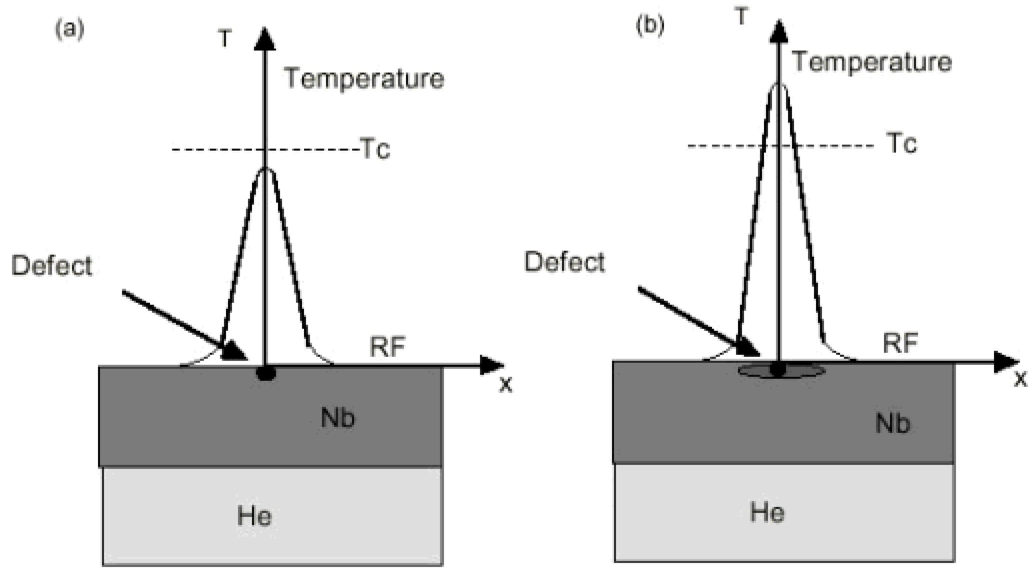

- Thermal breakdown occurs when the heat generated at the hot spot is larger than that can be evacuated to the helium bath

- Both the thermal conductivity and the surface resistance of Nb are highly temperature dependent between 2 and 9K

Losses in RF Cavities

Losses in Normal Conducting Cavities

- Losses are given by Ohm's Law $J = \sigma E$ where σ is the conductivity
- In a cavity, rf magnetic field drives an oscillating current in the cavity wall
- Following Maxwell's equations

$$\nabla \times \mathrm{B} = \mu j + \mu \varepsilon \frac{\partial \mathrm{E}}{\partial t} \qquad\qquad \nabla \times \mathrm{E} = -\frac{\partial \mathrm{B}}{\partial t}$$

- Neglecting displacement current

$$\nabla^2 \mathrm{B} - i\mu\sigma\omega \mathrm{B} = 0$$

Losses in Normal Conducting Cavities

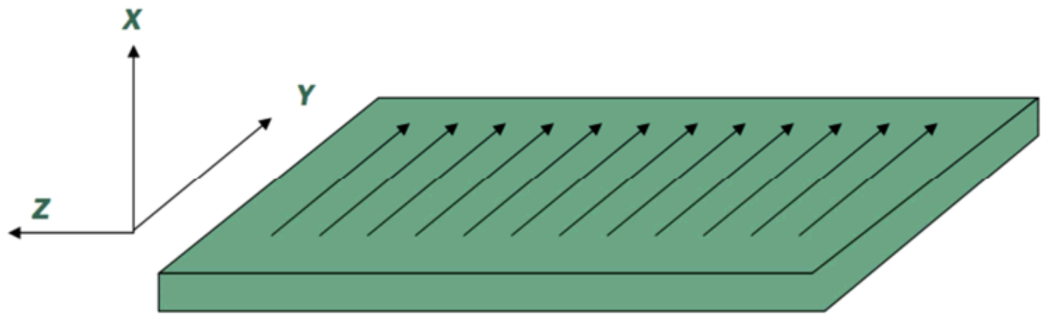

- Considering the cavity as wall as a local plane surface, solve one dimensional problem at the surface for uniform magnetic field in y direction

$$\nabla^2 B - i\mu\sigma\omega B = 0 \quad \Rightarrow \quad H_y = H_0 e^{-\frac{1+i}{\delta}x}$$

- with field decaying into the conductor over the skin depth

$$\delta = \left(\frac{2}{\mu_0 \omega \sigma} \right)^{1/2}$$

Losses in Normal Conducting Cavities

- From Maxwell equation $E_z = \dfrac{1+i}{\sigma\delta} H_y$
  - A small tangential electric field component decays into the conductor
- Surface impedance

$$H_y(z) = \frac{(1-i)}{\mu_0\,\omega\,\delta} E_z(z)$$

$$Z = \frac{E_z(0)}{H_y(0)} = \frac{(1+i)}{2}\mu_0\,\omega\,\delta = \frac{(1+i)}{\sigma\,\delta} = (1+i)\left(\frac{\mu_0\omega}{2\sigma}\right)^{1/2}$$

- Surface resistance is the real part of surface impedance

$$R_s = \frac{1}{\sigma\delta} = \sqrt{\frac{\mu_0\omega}{2\sigma}}$$

Superconductivity

- Superconductivity – Discovered in 1911 Kammerlingh-Onnes, is a phenomenon where below a certain temperature, called the critical temperature (T_c), some materials show a sudden drop of the dc electrical resistance to zero

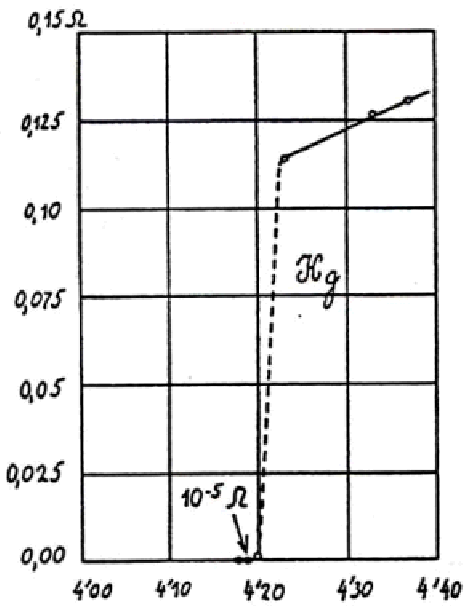

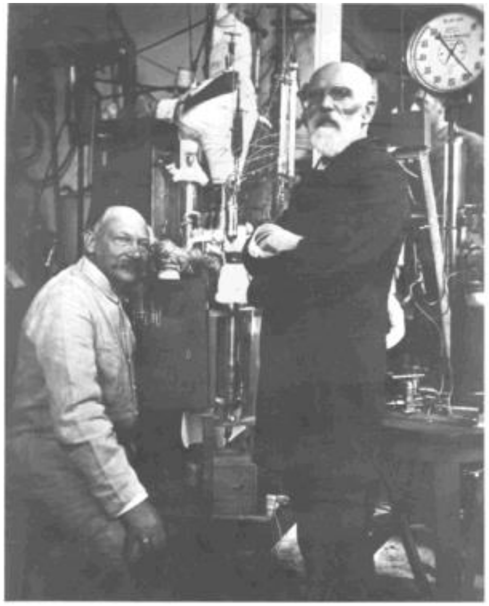

Kamerlingh Onnes and van der Waals in Leiden with the helium 'liquefactor' (1908)

Meissner Effect

Meissner Effect – Discovered by Meissner and Ochsenfeld in 1933

- Ability to completely expel an externally applied magnetic field when cooled down below the critical temperature (T_c)
- Superconductor behaves as a perfect diamagnet

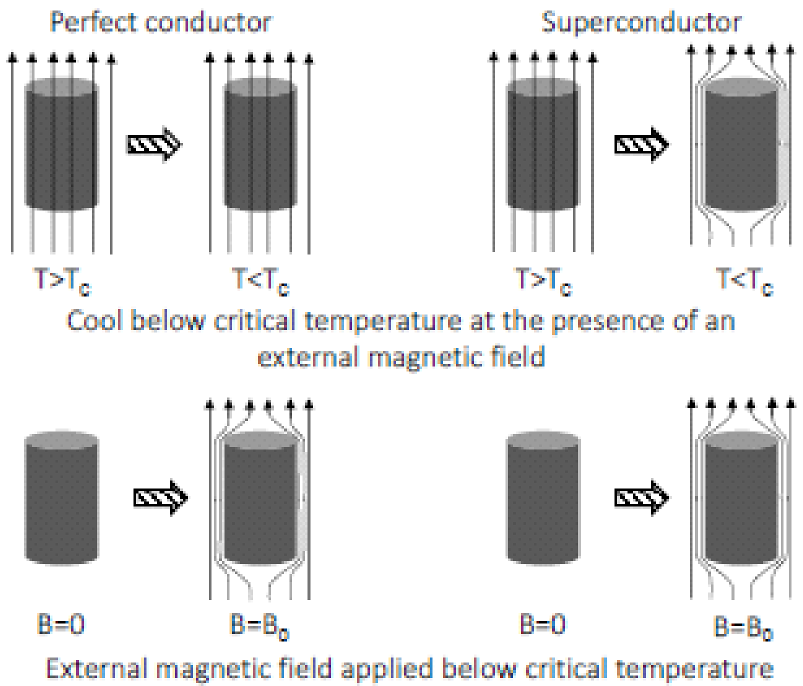

- Surface currents created at the surface generates a magnetic field that cancels the external magnetic field inside the superconductor
- These surface currents do not decay with time due to the zero resistance in the superconductor

Critical Magnetic Field

- Critical magnetic field (B_c) – Field beyond at which superconductivity is destroyed

$$B_c(T) = B_c(0)\left[1 - \left(\frac{T}{T_c}\right)^2\right]$$

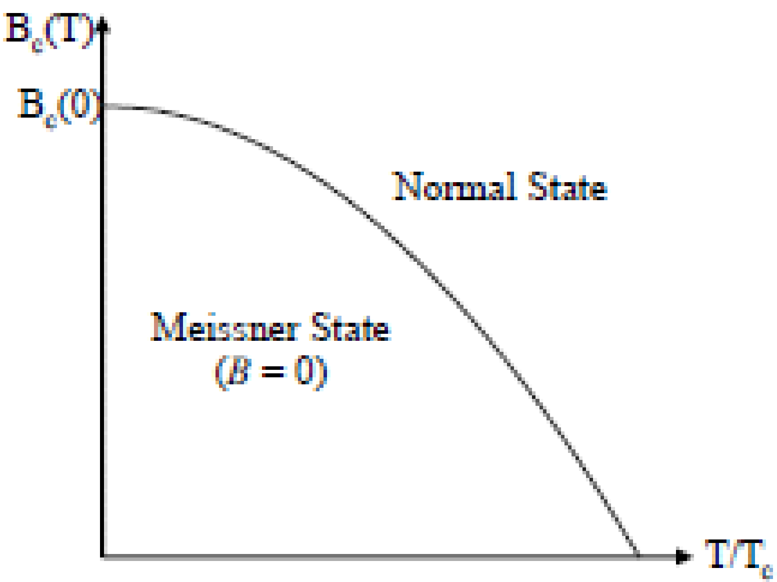

Type I – Soft Superconductors

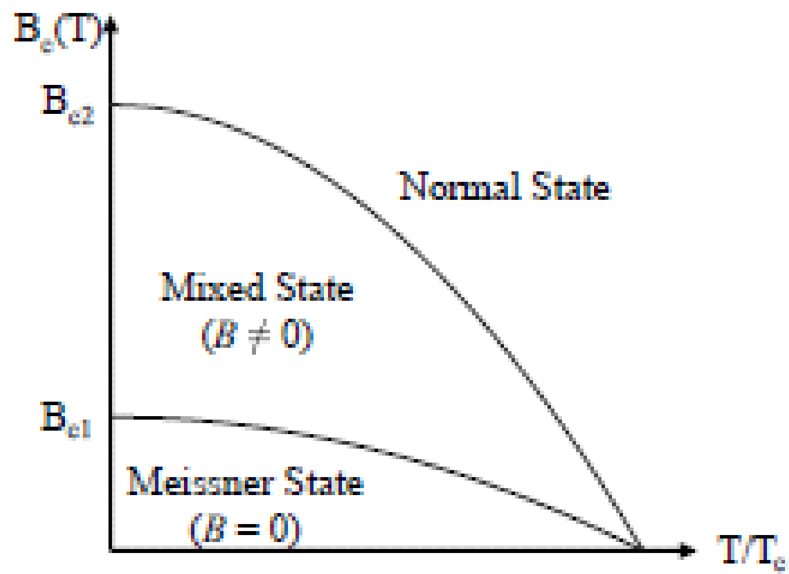

Type II – Hard Superconductors

Magnetization

- Meissner state in superconductor is an ideal diamagnet
- Magnetization: $(M = B - \mu_0 H)$

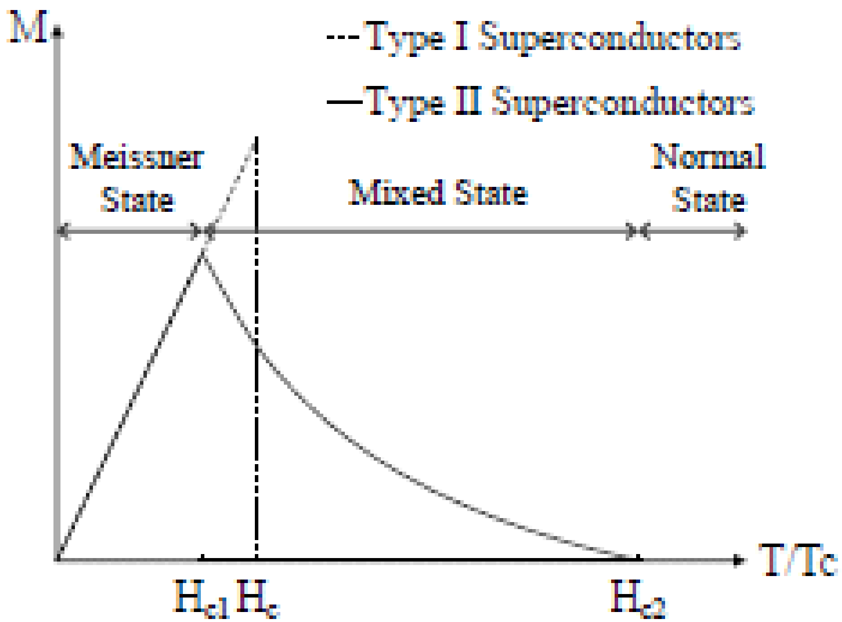

- Complete Meissner state - Type I superconductor
- Partial Meissner state – Type II superconductor

Theories of Superconductivity

- Gorter and Casimir (1934) – Two Fluid Model
  - London equations by F. London and H. London (1935) → London Penetration Depth (λ)
  - Non local generalization to London equations by Pippard → Pippard Coherence Length (ξ)

- Ginzburg Landau Theory (1950)
  - Second order phase transition of complex order parameter (Ψ)

- BCS Theory (Bardeen Cooper Schrieffer) (1957)
  - Microscopic theory
  - Two fluid mode revised

Two Fluid Model

- Macroscopic theory of superconductivity
- Coexistence of:
  - super electrons (n_s)
  - normal electrons (n_n)
  - Total density $n = n_s + n_n$
- Only super electrons are accelerated by the constant electric field (E) $m\frac{\partial \vec{v}_s}{\partial t} = e\vec{E}$
- Super current density $\vec{J}_s = -en_s\vec{v}$
- Yields <u>First London Equation</u> $\frac{\partial \vec{J}_s}{\partial t} = \frac{n_s e^2}{m}\vec{E}$
- Super electrons are not affected by the normal electrons $\vec{J}_n = \sigma_n \vec{E}$

London Equations

- Using Maxwell's equations

$$\vec{\nabla} \times \vec{E} = -\frac{\partial \vec{B}}{\partial t} \qquad \vec{\nabla} \times \vec{B} = \mu_0 \vec{J}_s$$

- Yield Second London Equation

$$\nabla^2 \vec{B} - \frac{\mu_0 n_s e^2}{m} \vec{B} = 0$$

- Field penetration in the superconductor

$$B(x) = B(0) exp\left[-\frac{x}{\lambda_L}\right]$$

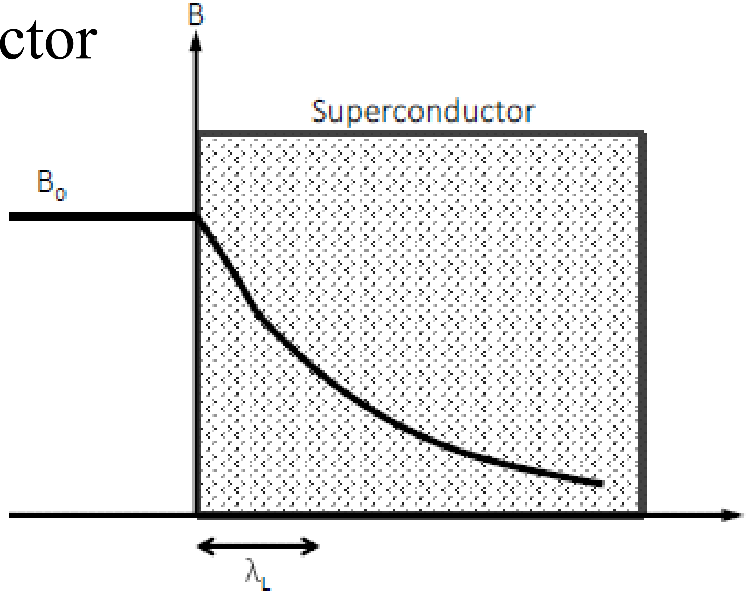

- **London penetration depth**

$$\lambda_L = \left[\frac{m}{\mu_0 n_s e^2}\right]^{1/2}$$

Fundamental Lengths

- London penetration depth (λ_L)
  - Distance over which magnetic fields decay in superconductors
- Pippard coherence length (ξ_0)
  - Distance over which the superconducting state decays

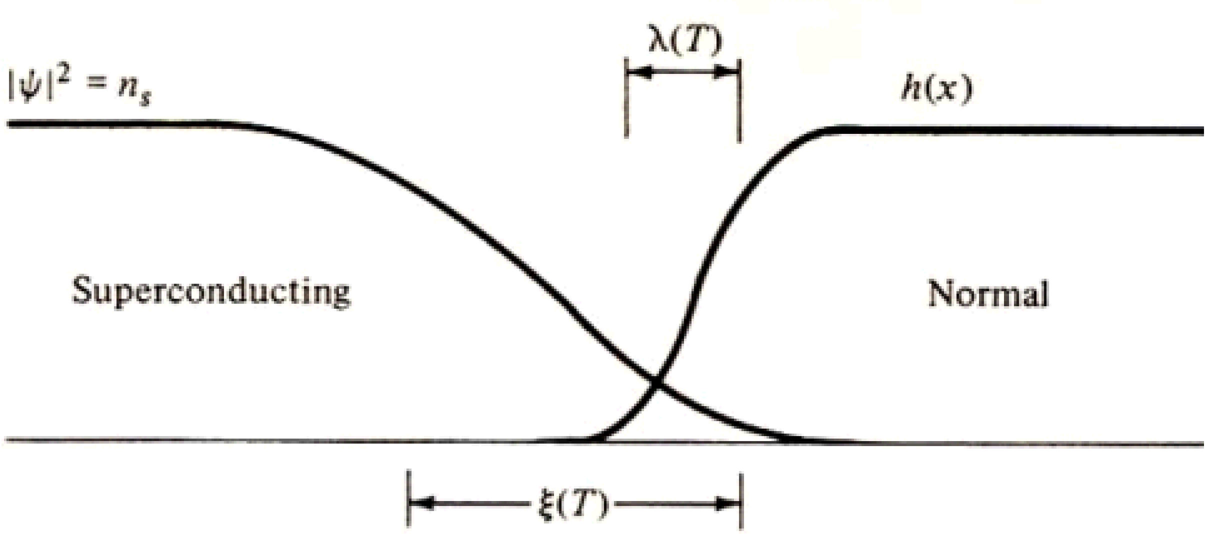

- Type II superconductors – $\lambda_L >> \xi_0$
- Type I superconductors – $\xi_0 >> \lambda_L$

Ginzburg Landau Theory

- Linear London equations

$$\frac{\partial \vec{J}_s}{\partial t} = -\frac{\vec{E}}{\lambda^2 \mu_0} \qquad \nabla^2 \vec{H} - \frac{1}{\lambda^2}\vec{H} = 0$$

- Describes the electrodynamics of superconductors at all T if:
  - Current density J_s is small
  - Density of super electrons (n_s) is spatially uniform
- Many important phenomena in superconductivity occur because (n_s) is not uniform
  - Interfaces between normal and superconductors
  - Trapped flux
  - Intermediate state
- G-L Theory – Nobel prize in 2003

Ginzburg Landau Theory

- G-L Theory – Generalization of London equations to nonlinear problems but still retain the local approximation of the electrodynamics

- Theory of second order phase transition is based on an order parameter which is zero above the transition temperature and non-zero below

- For superconductors, G-L theory uses a complex order parameter $\psi(r)$ such that $|\psi(r)|^2$ represents the density of super electrons

$$\psi\left(\vec{r}\right) = |\psi| exp\left(i\varphi\left(\vec{r}\right)\right)$$ $\varphi(r)$ is the phase

Ginzburg Landau Theory

- London penetration depth:

$$\lambda_L(T) = \left(\frac{m^*\beta}{2e^2\alpha'}\right)^{1/2}\sqrt{\frac{T_c}{T_c - T}}$$

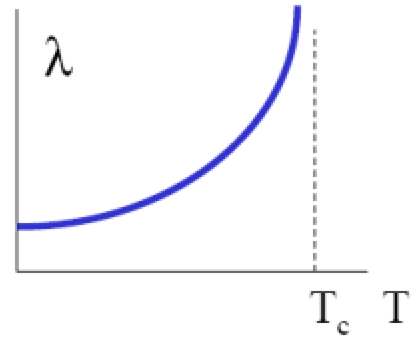

- Coherence length:

$$\xi(T) = \left(\frac{\hbar^2}{4m^*\alpha'}\right)^{1/2}\sqrt{\frac{T_c}{T_c - T}}$$

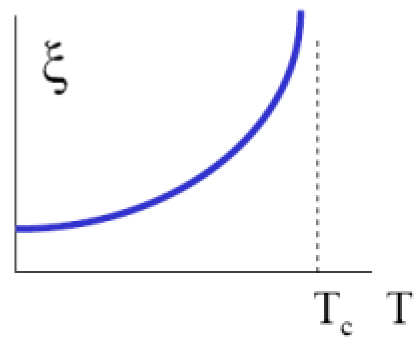

- GL parameter: $\kappa = \lambda(T)/\xi(T)$ is independent of T

- Critical field $H_c(T)$ $$H_c(T) = \frac{\phi_0}{2\sqrt{2}\,\xi(T)\,\lambda_L(T)}$$

Material Parameters

Superconductor	λ_L (0) (nm)	ξ_0 (nm)	κ	$2\Delta(0)/kT_c$	T_c(K)
Al	16	1500	0.011	3.40	1.18
In	25	400	0.062	3.50	3.3
Sn	28	300	0.093	3.55	3.7
Pb	28	110	0.255	4.10	7.2
Nb	32	39	0.82	3.5-3.85	8.95-9.2
Ta	35	93	0.38	3.55	4.46
Nb_3Sn	50	6	8.3	4.4	18
NbN	50	6	8.3	4.3	≤17
$Yba_2Cu_3o_x$	140	1.5	93	4.5	90

BCS Theory

- Bardeen-Cooper-Schrieffer Theory (1957) – Nobel prize in 1972
- Macroscopical → Microscopical representation

Low-Temperature Superconductivity

December was the 50th anniversary of the theory of superconductivity, the flow of electricity without resistance that can occur in some metals and ceramics.

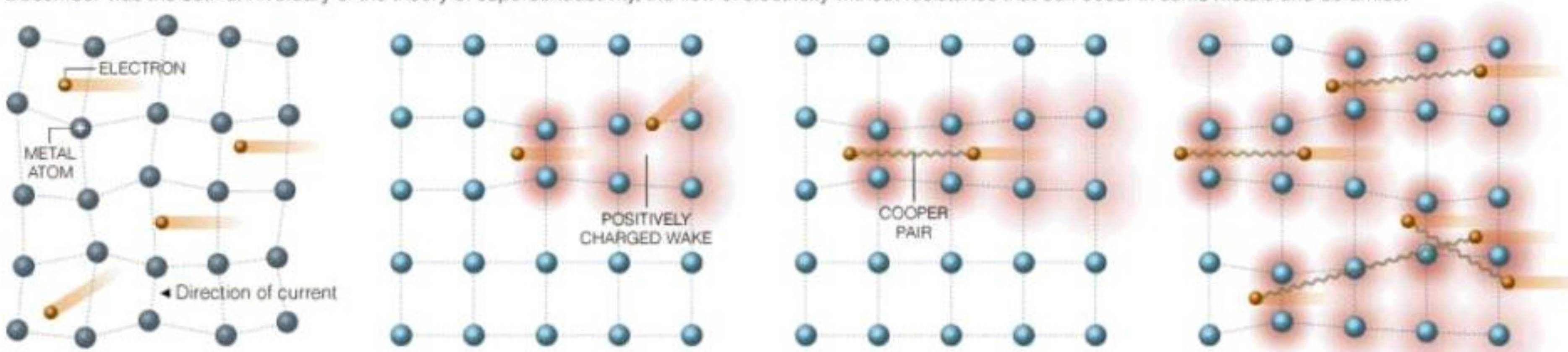

ELECTRICAL RESISTANCE
Electrons carrying an electrical current through a metal wire typically encounter resistance, which is caused by collisions and scattering as the particles move through the vibrating lattice of metal atoms.

CRITICAL TEMPERATURE
As the metal is cooled to low temperatures, the lattice vibration slows. A moving electron attracts nearby metal atoms, which create a positively charged wake behind the electron. This wake can attract another nearby electron.

COOPER PAIRS
The two electrons form a weak bond, called a Cooper pair, which encounters less resistance than two electrons moving separately. When more Cooper pairs form, they behave in the same way.

SUPERCONDUCTIVITY
If a pair is scattered by an impurity, it will quickly get back in step with other pairs. This allows the electrons to flow undisturbed through the lattice of metal atoms. With no resistance, the current may persist for years.

Sources: Oak Ridge National Laboratory; Philip W. Phillips

JONATHAN CORUM/THE NEW YORK TIMES

Cooper Pairs

- Cooper pairs – Pair of electrons formed due to electron-phonon interaction that dominates over the repulsive Coulomb force
- Moving electron distorts the lattice and leaves behind a trail of positive charge that attracts another electron moving in opposite direction
- Has lower energy than the two separate electrons
- Therefore, electron pairs form bound states of lower energy which are stable than the Fermi ground state
- Strong overlap of many Cooper pairs results in the macroscopic phase coherence

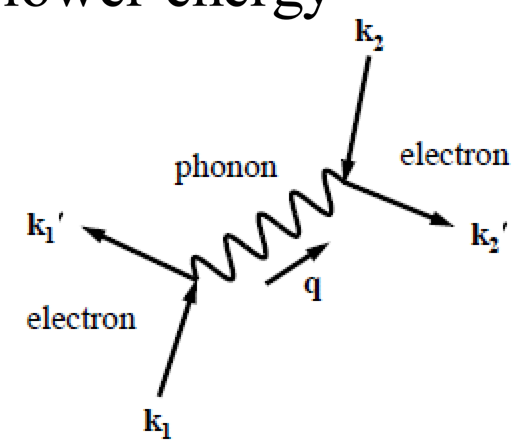

Energy Gap

- Energy gap (Δ) – gap around Fermi level between ground state and excited state

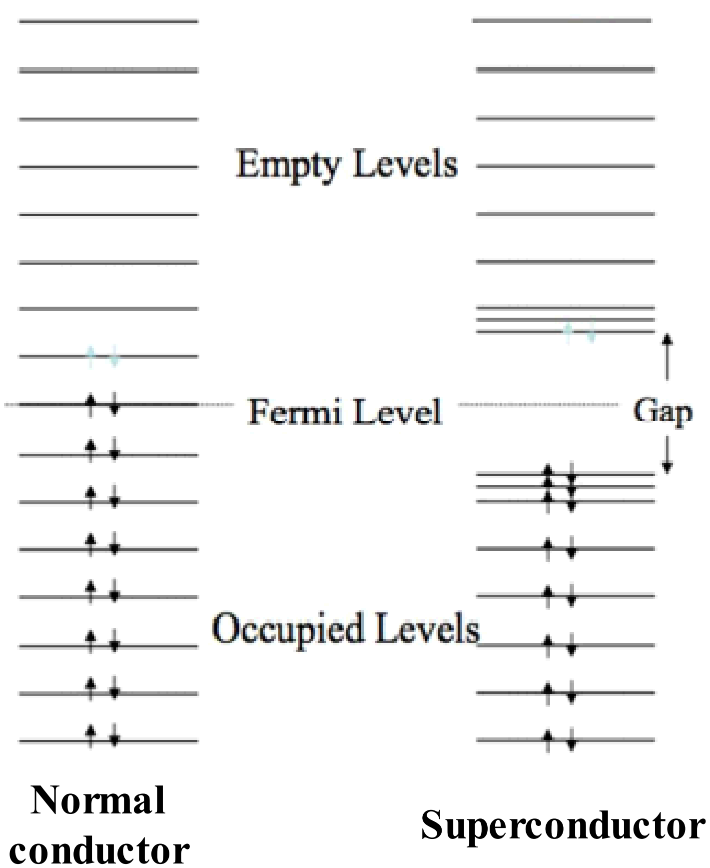

- At $0 < T < T_c$ not all electrons are bounded in to Cooper pairs
- Density of unpaired electrons is given by

$$n_{\text{normal}} \propto \exp\left(-\frac{\Delta}{k_B T}\right)$$

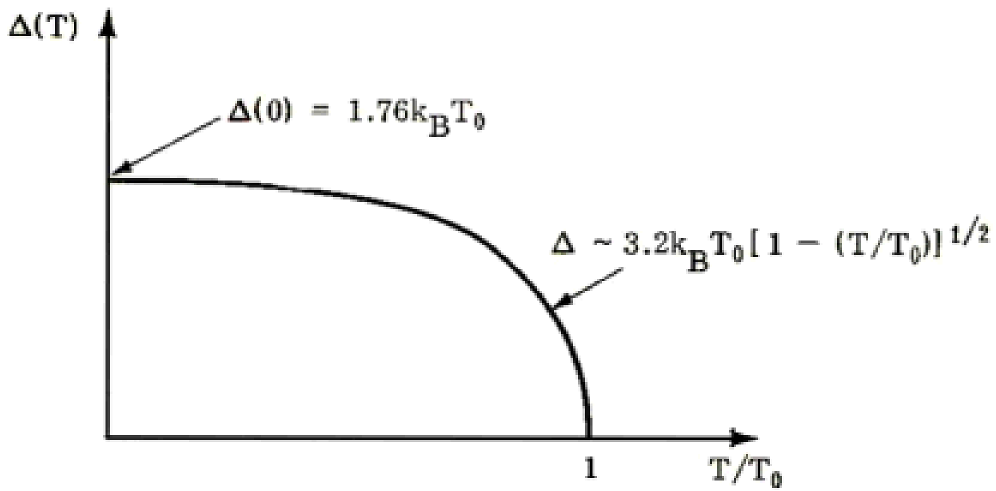

Losses in Superconductor

- At the presence of an rf field
  - Cooper pairs move without resistance → Do not dissipate power
  - Due to inertial mas of Cooper pairs they cannot follow an AC electromagnetic fields instantly and do not shield it perfectly
  - Remaining residual field accelerates the normal electrons that dissipate power
- More normal electrons → The material is more lossy
  - Losses decrease with temperature below T_c
- Faster the field oscillates the less perfect the shielding
  - Losses increase with frequency

Surface Impedance

- Following two fluid model

$$\vec{J}_s = \frac{n_e e^2}{m\omega}\vec{E} \qquad \vec{J}_n = -\frac{i}{\mu_0 m \lambda_L^2}\vec{E}$$

- Total current density $\vec{J} = \vec{J}_n + \vec{J}_s = (\sigma_n - i\sigma_s)\vec{E}$
- Surface Impedance: $Z_s = \sqrt{\frac{\omega\mu_0}{\sigma}}(1+i)$

- Skin depth

$$\delta = \sqrt{\frac{2}{\omega\mu_0\sigma}} = \sqrt{\frac{2}{\omega\mu_0(\sigma_n - i\sigma_s)}} \approx (1+i)\lambda_L\left(1+i\frac{\sigma_n}{2\sigma_s}\right)$$

$$H_y = H_0\, e^{-x/\lambda_L}\, e^{-ix\sigma_n/2\sigma_s\lambda_L}$$

BCS Surface Resistance

- Surface impedance $$Z_s \approx \sqrt{\frac{\omega\mu_0}{\sigma_s}}\left(\frac{\sigma_n}{2\sigma_s}+i\right) = R_s + iX_s$$

$$X_s = \omega\mu_0\lambda_L \qquad R_s = \frac{1}{2} \approx \sigma_n\omega^2\mu_0^2\lambda_L^3$$

- Taking may parameters into account Mattis and Bardeen developed theory based on BCS theory

$$R_{BCS} = A\frac{\omega^T}{T}\exp\left(\frac{-\Delta}{k_B T}\right)$$

A – material parameters

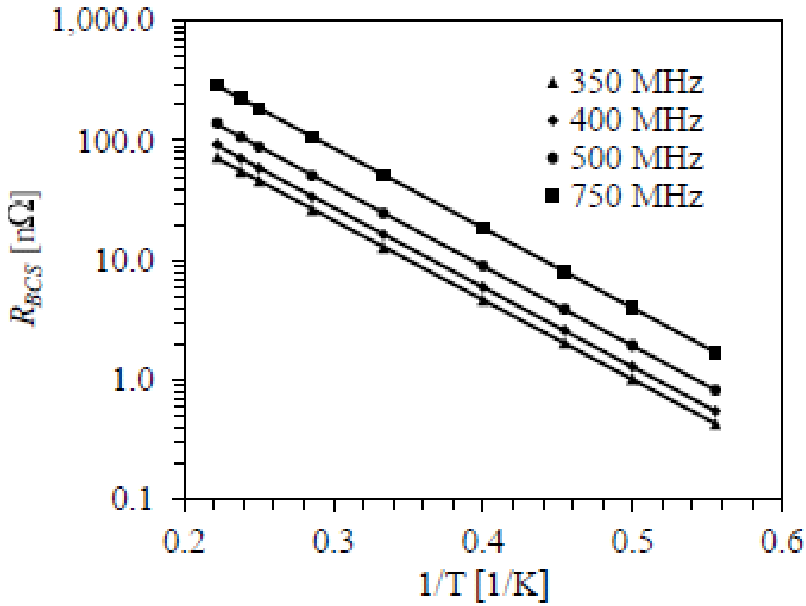

Surface Resistance

- Surface resistance of superconductors (R_s)

$$R_s = R_{BCS} + R_{res} \quad [\Omega]$$

- Residual resistance (R_{res}) due to:
  - Dielectric surface contaminants (gases, chemical residues, ..)
  - Normal conducting defects, inclusions
  - Surface imperfections (cracks, scratches, ..)
  - Trapped flux during cool down through critical temperature
  - Hydrogen absorption during chemical processing

- An approximation of R_{BCS} for Nb:

$$R_{BCS} \approx 2\times10^{-4}\left(\frac{f\,[\mathrm{GHz}]}{1.5}\right)^2 \frac{1}{T}\exp\left(\frac{-17.67}{T}\right) \quad [\Omega]$$